



## Research paper

# Synthesis and optimization of novel allylated mono-carbonyl analogs of curcumin (MACs) act as potent anti-inflammatory agents against LPS-induced acute lung injury (ALI) in rats



Heping Zhu<sup>a,1</sup>, Tingting Xu<sup>a,b,1</sup>, Chenyu Qiu<sup>a,1</sup>, Beibei Wu<sup>a,b</sup>, Yali Zhang<sup>a</sup>,  
Lingfeng Chen<sup>a</sup>, Qinqin Xia<sup>a</sup>, Chenglong Li<sup>a</sup>, Bin Zhou<sup>b,\*\*</sup>, Zhiguo Liu<sup>a,\*</sup>, Guang Liang<sup>a</sup>

<sup>a</sup> Chemical Biology Research Center at School of Pharmaceutical Sciences, Wenzhou Medical University, 1210 University Town, Wenzhou, Zhejiang, 325035, China

<sup>b</sup> The Second Affiliated Hospital, Wenzhou Medical University, Wenzhou, Zhejiang, 325035, China

## ARTICLE INFO

## Article history:

Received 15 December 2015

Received in revised form

18 May 2016

Accepted 19 May 2016

Available online 21 May 2016

## Keywords:

Acute lung injury

Water solubility

Chemical stability

Drug design

Mono-carbonyl analogs of curcumin

## ABSTRACT

A series of novel symmetric and asymmetric allylated mono-carbonyl analogs of curcumin (MACs) were synthesized using an appropriate synthetic route and evaluated experimentally through the LPS-induced expression of TNF- $\alpha$  and IL-6. Most of the obtained compounds exhibited improved water solubility as a hydrochloride salt compared to lead molecule **8f**. The most active compound **7a** was effective in reducing the Wet/Dry ratio in the lungs and protein concentration in bronchoalveolar lavage fluid. Meanwhile, **7a** also inhibited mRNA expression of several inflammatory cytokines, including TNF- $\alpha$ , IL-6, IL-1 $\beta$ , and VCAM-1, in Beas-2B cells after Lipopolysaccharide (LPS) challenge. These results suggest that **7a** could be therapeutically beneficial for use as an anti-inflammatory agent in the clinical treatment of acute lung injury (ALI).

© 2016 Elsevier Masson SAS. All rights reserved.

## 1. Introduction

Acute lung injury (ALI) is an infrequent but potentially life-threatening illness in critically ill patients [1,2]. Histologically, ALI in humans is characterized by a severe acute inflammatory response in the airspaces and lung parenchyma. Major pathological changes include neutrophil accumulation, inflammatory mediator production, increased vascular permeability, parenchymal injury and severely impaired gas exchange [3–5]. Several studies indicate that some inflammatory factors associated with lung injury, such as Interleukin (IL)-6, IL-1 $\beta$ , and tumor necrosis factor (TNF)- $\alpha$ , but the underlying mechanisms of ALI mediated by these inflammatory factors are still uncertain [6–8]. Despite recent advances in many new treatment strategies, the mortality of ALI still remains more

than 40% [9,10]. Thereby, the development of novel agents for treatment of ALI is still urgently needed.

Curcumin, a yellow substance derived from the rootstalk of the turmeric plant (*Curcuma longa*), has been extensively investigated for its anti-inflammatory activity [11–13], chemopreventative and anti-tumor properties [14–16]. However, its poor aqueous solubility and relatively low bioavailability, have been highlighted as major limitation for application as revealed in phase I/II studies [17,18]. We previously synthesized a series of novel mono-carbonyl analogs of curcumin (MACs), deleting  $\beta$ -diketone moiety and having allylic and prenylic substituents at different positions showing potential anti-inflammatory activities (Fig. 1) [19]. Some of our molecules, such as compound **8f**, significantly enhanced chemical stability and exhibited effective protection against LPS-induced death in septic mice. Unfortunately, as with many other curcumin derivatives, they continued to have a low water solubility and incomplete structure-activity relationship (SAR) data.

In an ongoing effort to develop novel anti-inflammatory therapeutics, we hypothesized that the piperidone system containing a nitrogen-atom in compounds may play important roles in their solubility by conversion to the salt form. Additionally, optimization

\* Corresponding author.

\*\* Corresponding author. The Department of Hepatobiliary Surgery, The Second Affiliated Hospital of Wenzhou Medical University, Wenzhou, Zhejiang, 325035, China.

E-mail addresses: [pzhoubin@sina.com](mailto:pzhoubin@sina.com) (B. Zhou), [lzgcnu@163.com](mailto:lzgcnu@163.com) (Z. Liu).

<sup>1</sup> These authors contribute equally to this work.

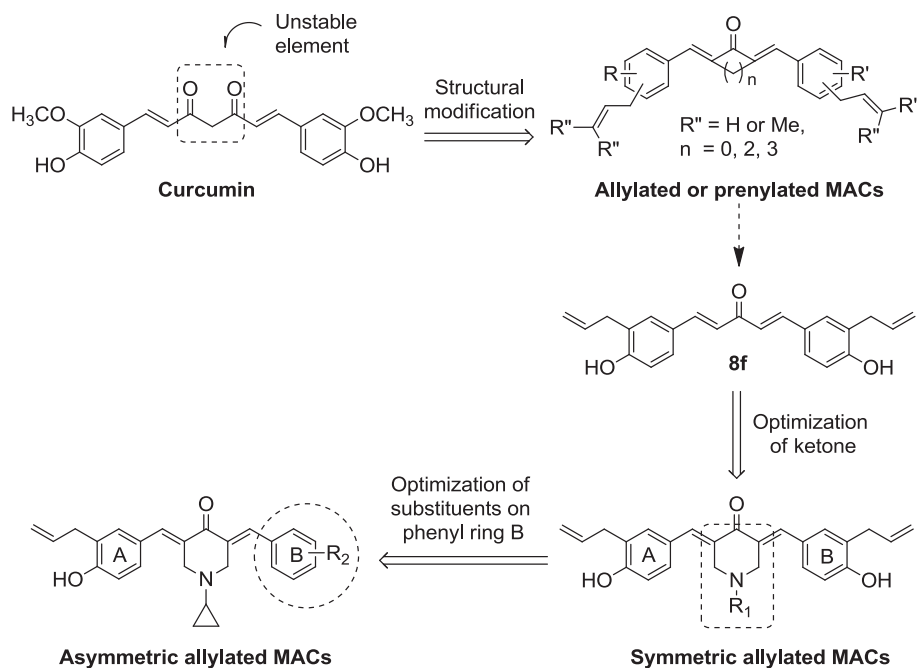


Fig. 1. Chemical structures of **8f** and structural design of new allylated MACs.

one of phenyl substituents may provide new lead compounds with enhanced activity, as well as better solubility. In the present investigation, we designed and synthesized a series of novel allylated MACs containing a piperidone fragment based on the **8f** chemical structure in order to pursue and develop novel anti-inflammatory agents. To the best of our knowledge, this type of curcumin derivatives has not been previously synthesized. Importantly, active compound **7a** showed improved anti-inflammatory activities *in vitro* and significant therapeutic effects *in vivo*, suggesting the potential of allylated MACs for development as a new anti-inflammatory agent for the treatment of ALI.

## 2. Chemistry

The titled compounds were synthesized by following a multi-step synthesis protocol. As shown in Scheme 1, allylation of commercially available 4-Hydroxybenzaldehyde (**1**) obtained 4-(allyloxy)benzaldehyde (**2**), which was subjected to a key Claisen rearrangement in order to give the 3-allyl-4-hydroxybenzaldehyde **3** in about 30% overall yield. With a rearrangement product of **3** in hand, it was treated with various substituted piperidones in a catalyst of hydrogen chloride gases, which furnished targeted symmetric allylated MACs **4a–l** at a 30–40% yield. However, it is difficult to prepare the intermediate ketone for the production of asymmetric MACs by using acidic condition. Therefore, we here develop an attractive approach to obtain the desired asymmetric molecules under the alkaline reaction conditions. Protection of 3-allyl-4-hydroxybenzaldehyde **3** with 3,4-dihydro-2H-pyran afforded O-THP protected benzaldehyde **5** in a quantitative yield. Aldol condensation of benzaldehyde **5** with *N*-cyclopropyl-4-piperidinone in the presence of pyrrolidine afforded  $\alpha,\beta$ -unsaturated ketone **6**, which was further subjected to condensation using different benzaldehydes, followed by THP-deprotection to give the asymmetric allylated MACs **7a–e** with a 25–30% overall yield. In the process of synthesis, the yields of symmetrical analogs were higher than the asymmetric analogs. The physicochemical parameters of the synthesized compounds are presented in Table 1. The

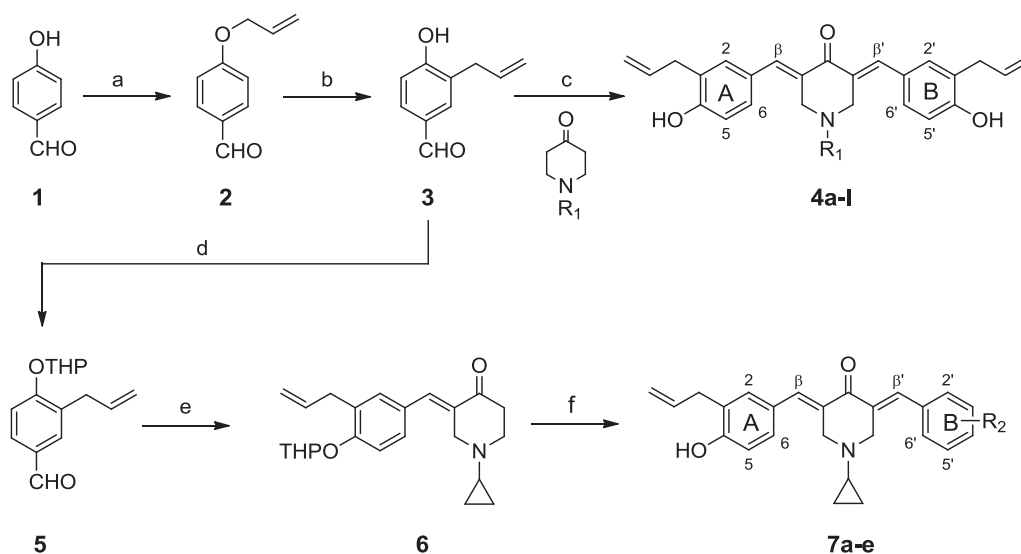
analytical and spectral data of the final compounds are in full agreement with the proposed structures.

## 3. Results and discussion

### 3.1. Anti-inflammatory screening and structure-activity relationship studies

TNF- $\alpha$  and IL-6 are two well-known pro-inflammatory cytokines. It has been well demonstrated that they contribute to the initiation and extension of an inflammatory-induced ALI process [20,21]. To determine whether new allylated MACs have any inhibitory effects in ALI treatment, their ability to reduce LPS-stimulated TNF- $\alpha$  and IL-6 release was determined in mouse macrophages. After pretreatment with 10  $\mu$ M compounds for 30 min, macrophages were treated with 0.5 mg/mL LPS for 24 h. The levels of TNF- $\alpha$  and IL-6 in culture medium were determined by enzyme-linked immunosorbent assay (ELISA) and normalized to the total protein amounts of the viable cell pellets.

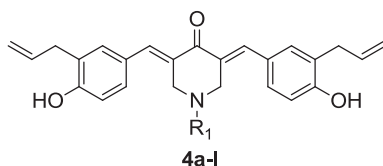
We first investigated the influence of the N-substituents on the piperidone. Thirteen symmetrical allylated MACs were evaluated for their anti-inflammatory activity, and the results are summarized in Table 1. Initial screening showed that a majority of these compounds exhibited effective inhibition against LPS-stimulated IL-6, but almost no activity toward TNF- $\alpha$ , except for compound **4f** with an inhibition ratio of 39.4%. In comparison with positive control compound **8f** (% inhibition = 59.6%), the potency of compound **4a** possessing an unsubstituted piperidone motif was not improved for IL-6 inhibition. However, incorporation of various alkyl groups, such as methyl, ethyl, propyl, isopropyl and cyclopropyl on the nitrogen atom, yielded compounds **4b–f**, respectively. These compounds displayed substantial improvement in IL-6 inhibitions relative to **4a**. Benzylation of the nitrogen atom gave compound **4h**, which had a similar activity (%inhibition = 45.8%), but benzenesulfonylation provided compound **4g** (% inhibition = 24.8%), which had a lower activity than compound **4a**. Interestingly, introduction of various benzyloxy groups at the



**Scheme 1.** General synthetic routes for **4a–l** and **7a–e**. Reagents and conditions: (a) allyl bromide,  $K_2CO_3$ , acetone, 65 °C, 10 h, 75%; (b) *N,N*-diethylaniline, 200 °C, 5 h, 40%; (c) HCl(gas), HAc, rt, two days, 30–40%; (d) 3,4-dihydro-2*H*-pyran, PPTS, 8 h,  $CH_2Cl_2$ , 40 °C, 85%; (e) 1-Cyclopropylpiperidin-4-one, pyrrolidine,  $CH_2Cl_2$ , 40 °C, 4 h, 40%; (f) i) various benzaldehydes, EtOH, 20% (w/v) NaOH, rt, overnight, 25–30%, ii) 1 mol/L HCl, EtOH, rt, 5 h, 100%.

**Table 1**

Chemical structures and SAR of symmetric allylated MACs **4a–l**.



Comp.	$R_1$	clogP <sup>a</sup>	(% inhibition (10 nM))		HL7702 cell survival rate (%)
			IL-6	TNF- $\alpha$	
<b>4a</b>	–H	3.76	44.36 ± 9.4 <sup>b</sup>	N.A <sup>c</sup>	77.89 ± 0.79
<b>4b</b>	–Me	4.45	57.14 ± 7.9	N.A	80.35 ± 2.1
<b>4c</b>	–Et	4.81	67.62 ± 3.2	N.A	79.60 ± 1.2
<b>4d</b>	–Pr	5.03	76.14 ± 2.5	N.A	75.16 ± 1.9
<b>4e</b>	– <i>iso</i> –Pr	5.30	71.59 ± 4.3	N.A	85.08 ± 1.1
<b>4f</b>	– <i>c</i> –Pr	4.89	77.54 ± 4.7	39.49 ± 8.1	76.18 ± 1.2
<b>4g</b>	–SO <sub>2</sub> –Ph	4.83	24.75 ± 18.9	N.A	63.39 ± 6.9
<b>4h</b>	–Bz	5.46	45.84 ± 12.6	N.A	62.12 ± 4.8
<b>4i</b>	–CO-(2',6'–Cl)Ph	6.59	79.64 ± 6.1	N.A	79.64 ± 6.1
<b>4j</b>	–CO-(4'–F)Ph	5.35	86.85 ± 5.6	N.A	77.96 ± 7.3
<b>4k</b>	–CO-(4'–Cl)Ph	5.89	89.23 ± 6.7	N.A	66.25 ± 3.9
<b>4l</b>	–CO-(4'–Me)Ph	5.69	81.48 ± 3.9	N.A	70.13 ± 2.3
<b>8f</b>		5.89	59.59 ± 4.9	7.15 ± 9.3	73.28 ± 2.2

<sup>a</sup> Calculated logP (clogP) value at <http://146.107.217.178/lab/alogps/start.html>.

<sup>b</sup> Each value represents mean ± SD of three experiments.

<sup>c</sup> not determined.

nitrogen atom in compound **4a** produced compound **4i–l**, and led to more potent IL-6 inhibition at an inhibition rate ranging from 79.6% to 89.2%. On the basis of these results, it appeared that a bulky lipophilic alkyl group or benzyloxy group, may have a favorable inhibitory effect against IL-6 production.

In order to examine whether the substitution of moiety groups affected biological activities of newly synthesized analogs, the octanol partition coefficient value (ClogP, see Table 1) of each compound was calculated using ALOGPS 2.1 program [22]. The results revealed that analogs **4b–f** and **4i–l** containing *N*-alkyl substituents or *N*-benzyloxy moieties at the piperidine, provided more improvements in both hydrophilicity and potency contrasted to

that of the control **8f**. However, the nature (**4a**) and *N*-benzyl group (**4h**) of piperidine greatly decreased their IL-6 potency, even if compound **4a** provides the lowest hydrophobicity (ClogP = 3.76). Again, the cytotoxicity and safety of synthetic MACs were tested in a human normal hepatic cell line (HL-7702 cells). Cell viability was detected by MTT assay after treatment with the compounds for 24 h. As shown in Table 1, only **4g**, **4h** and **4k** showed moderate cytotoxicity (survival rates < 70%), while the other compounds were nontoxic at 10  $\mu$ M in RAW264.7 cells, indicating that they are relatively safe.

To develop anti-inflammatory compounds that both strongly decreased LPS-induced IL-6 and TNF- $\alpha$  releases, while enhancing

their water-solubility and to further explore the structure-activity relationship (SAR), we next directed our optimization effort to modification of the phenol ring by introduction of various hydrophilic groups. Compound **4f** was selected as a lead compound after the initial screening which showed potential inhibition in LPS-secreted IL-6 and TNF- $\alpha$ .

Table 2 illustrates that experimental and calculated logP values of compounds **7a–e** had no significant improvement relative to **4f** [23]. We suspected that strong intermolecular crystal packing forces and hydrophobic interactions may contribute to their low ClogP values. However, their hydrochloride salts showed a marked increase in aqueous solubility, especially for compounds **7a**, **7b**, and **7e**, which provided an experimental solubility of more than 17.0 mg/mL. Of all the compounds, 4-methyl piperidiny **7a** showed the strongest inhibitory activity on LPS-induced IL-6 and TNF- $\alpha$  production, with inhibitory rates of 83.3% and 43.8%, respectively. However, replacement of 4-methyl piperidiny with morpholinyl (**7b**) and the pyrrolidinyl (**7c**) lowered the potency compared to **7a**. Moreover, *N,N*-diethyl **7d** and *N,N*-dimethyl **7e**, exhibited a moderate inhibition with its inhibitory rates reaching 71.9%, 74.4% for IL-6, and 32.2%, 35.0% for TNF- $\alpha$ , respectively. Interestingly, the HL7702 survival rates of compounds **7a–e** reached a range of 89.4–95.5%, which was significantly higher than that of **4f**, reconfirming the safety of the tested compounds *in vitro*. Overall, compound **7a** was the only molecule with a well-balanced *in vitro* pharmacological profile and was thus selected for further biological characterization.

### 3.2. Active compounds inhibit LPS-induced cytokine release in a dose dependent manner

To further evaluate dose-dependent inhibitory effects of active compounds, RAW264.7 macrophages were pretreated with **4f** and **7a** at indicated concentrations (1, 2.5, 5, 10  $\mu$ M) for 30 min, and subsequently incubated with or without LPS (0.5  $\mu$ g/mL) for 24 h. Accordingly, the previously reported compound **8f** was applied at a concentration of 10  $\mu$ M as a treatment positive control. The release of inflammatory cytokines into the culture medium was determined by ELISA. As shown in Fig. 2A and B, active compound **7a** and its lead **4f**, exhibited a dose-dependent inhibition on both TNF- $\alpha$  and IL-6 releases induced by LPS. Furthermore, among the tested

compounds, **7a** gave indications as being the most promising and mostly equal to **4f** in activity for inhibition of IL-6 and TNF- $\alpha$  expression, at a concentration of 10  $\mu$ M, respectively. These results suggest that **7a** may be a potential candidate compound for development as an anti-inflammatory agent. Therefore, **7a** was selected for further testing against cytokine-mediated acute lung injury.

### 3.3. Chemical stability of representative curcumin derivatives

The widespread clinical application of curcumin has been limited due to its instability and poor metabolism. In one of our early publications, we reported MACs **8f** as one of the most stable compounds in a phosphate buffer (pH 7.4). Herein, we examined the stability of active compound **7a** under the same experimental conditions. As shown in Fig. 3A, 50% of the curcumin degraded within 25 min at the maximum absorbance of 425 nm. This finding is generally consistent with curcumin instability and a poor metabolic property. However, three allylated MACs **8f** with its derivatives **4f** and **7a**, demonstrated almost complete stability under the same condition (Fig. 3B–D). Overall, these result showed that the modified MACs are chemically more stable than curcumin *in vitro*.

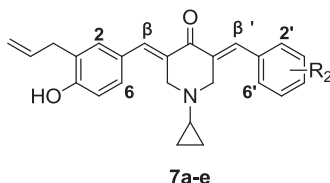
### 3.4. Effect of **7a** on survival of rats with LPS-induced ALI

We further investigated whether the active compound **7a** could prevent LPS-induced death *in vivo*. Thus rats were intraperitoneally injected with LPS 20 mg/kg after an intravenous injection of 10 mg/kg hydrochloride salt of **7a**, and the survival rate was monitored for 7 days. As shown in Fig. 4, all 10 animals that received saline died within 36 h in the LPS group. Only 50% of rats pretreated with **7a** at 10 mg/kg died after LPS challenge. The overall difference in survival rate between groups with and without **7a** was significant ( $p < 0.01$ ).

### 3.5. Effects of **7a** on pathophysiologic changes of lung in LPS-induced ALI rats

Allylated MAC **7a** showing the highest anti-inflammatory activity was chosen for the next evaluation in rats with ALI induced by intratracheal instillation of LPS. The details of animal experiments

**Table 2**  
Chemical structures and SAR of asymmetric allylated MACs **7a–e**.



Comp.	R <sub>2</sub>	clogP <sup>a</sup>	logP <sup>b</sup>	S <sub>drug</sub> <sup>c</sup> (mg/mL)	(% inhibition (10 $\mu$ M))		HL7702 cell survival rate (%)
					IL-6	TNF- $\alpha$	
7a	4'-Methylpiperazine	4.41	3.48	22.5	83.26 $\pm$ 4.0 <sup>d</sup>	43.81 $\pm$ 2.1	90.29 $\pm$ 6.1
7b	4'-Morpholine	4.44	3.21	19.4	59.83 $\pm$ 6.1	8.19 $\pm$ 6.6	94.30 $\pm$ 2.8
7c	4'-Pyrrole	5.10	4.33	N.D. <sup>e</sup>	49.86 $\pm$ 4.0	17.56 $\pm$ 3.6	95.50 $\pm$ 3.8
7d	4'-N(Et) <sub>2</sub>	5.62	4.08	N.D.	71.94 $\pm$ 3.6	32.15 $\pm$ 3.1	94.05 $\pm$ 6.5
7e	4'-N(Me) <sub>2</sub>	4.72	3.50	17.1	74.40 $\pm$ 5.1	34.99 $\pm$ 3.3	89.39 $\pm$ 2.0

<sup>a</sup> Calculated logP (clogP) value at <http://146.107.217.178/lab/alogps/start.html>.

<sup>b</sup> LogP data refers to experimental values observed for the selected compound in a previous paper.

<sup>c</sup> Aqueous kinetic solubility at pH 7.4.

<sup>d</sup> Each value represents mean  $\pm$  SD of three experiments.

<sup>e</sup> not determined.

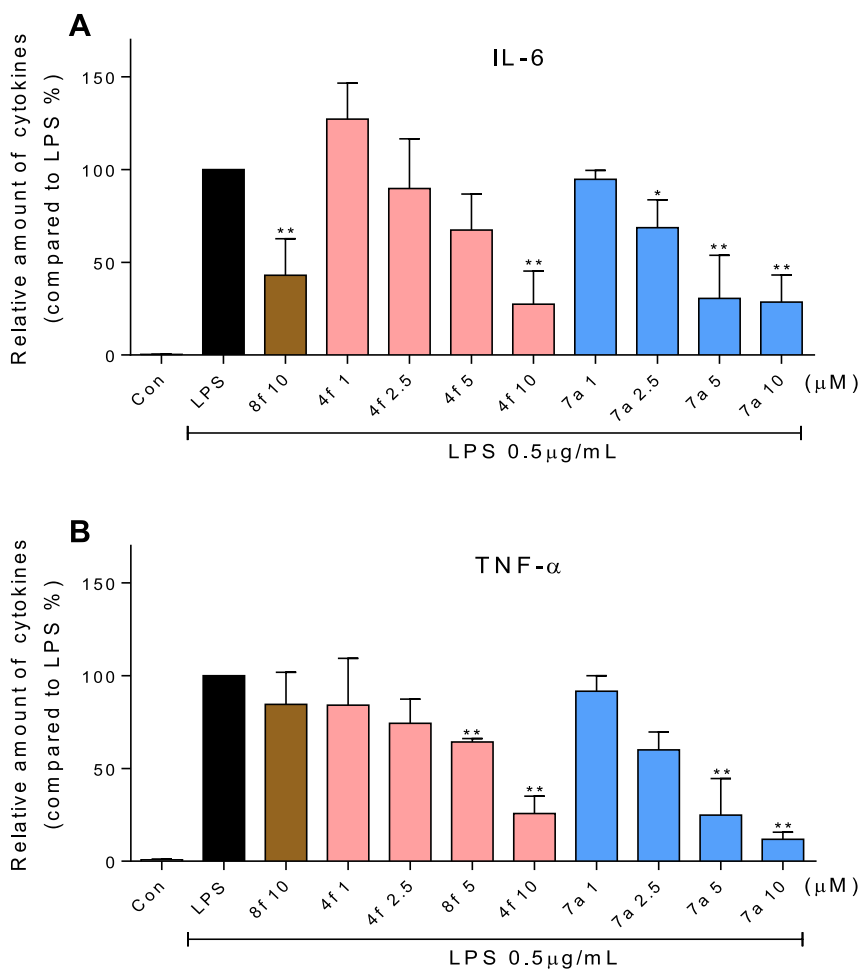


**Fig. 2.** Active MACs **4f** and **7a** inhibited LPS-induced IL-6 release in a dose-dependent manner. Macrophages were plated at a density of  $4.0 \times 10^5$ /plate overnight in 37 °C and 5% CO<sub>2</sub>. Cells were pretreated with active compounds in a series concentration of 1 μM, 2.5 μM, 5 μM and 10 μM for 30 min and subsequently incubated with or without LPS (0.5 μg/mL) for 24 h (A) IL-6 and (B) TNF-α levels in the culture medium were measured by ELISA and were normalized by the total protein. The results were presented as the percent of LPS control. Each bar represents the mean ± SEM of the three independent experiments. Statistical significance relative to the LPS group was indicated, \*p < 0.05; \*\*p < 0.01.

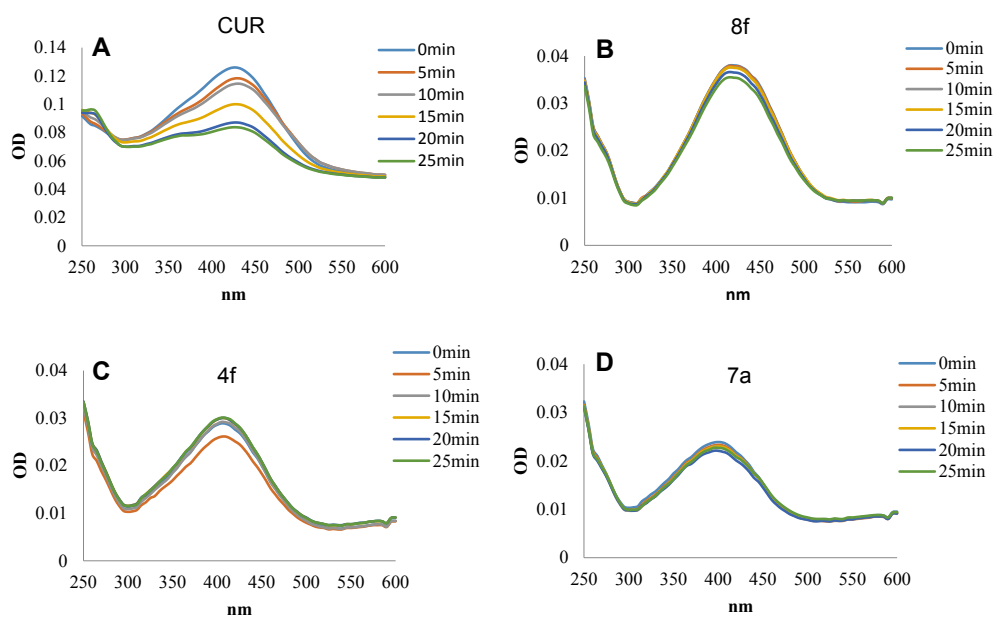


**Fig. 3.** Ultraviolet–visible absorption spectra of curcumin (A), **8f** (B), **4f** (C), and **7a** (D) in phosphate buffer (pH 7.4) containing 5% dimethyl sulfoxide.

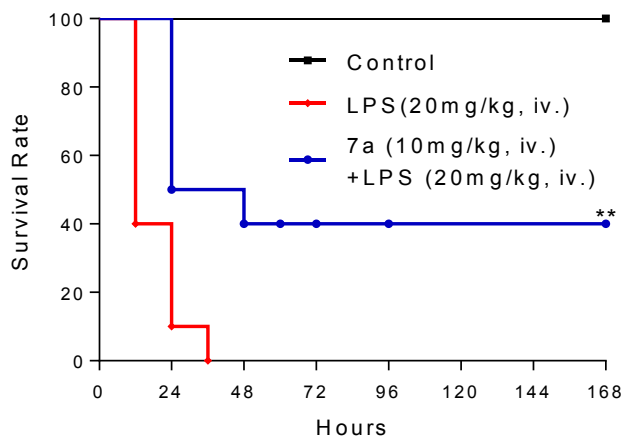


**Fig. 4.** Allylated MAC **7a** attenuated LPS-induced septic shock *in vivo*. Male C57BL/6 mice were pretreated with **7c** (IV, 10 mg/kg) or vehicle, followed by the injection of LPS (IP, 20 mg/kg). The survival rate was recorded for 7 days at an interval of 24 h after the LPS injection;  $n = 10$  animals in each group.

are described in the experimental section. The results indicated that the lung Wet/Dry ratio (W/D ratio, Fig. 5A) and the total protein concentration (Fig. 5B) significantly increased in the bronchoalveolar lavage fluid (BALF) of ALI rats at 6 h after LPS challenge, compared to those of the control group. Pretreatment with **7a** at 10 and 20 mg/kg, was found to significantly decrease the lung W/D ratio and the total protein concentration in BALF, respectively.

To evaluate histological changes after **7a** treatment in LPS-treated rats, lung sections were subjected to hematoxylin and eosin staining. Lung tissues from the control group showed a normal structure and no histopathological change under a light microscope (Fig. 5C). LPS instillation resulted in a significant pro-inflammatory alterations characterized by lung edema, alveolar hemorrhage, inflammatory cell infiltration, and destruction of epithelial and endothelial cell structure. However, these histopathological changes were ameliorated using 10 and 20 mg/kg of **7a**. These results indicated that modified MAC **7a** had a remarkable

protective effect for lung-based injury in a rat model of ALI.

### 3.6. Effect of **7a** on pulmonary inflammation of lung in LPS-stimulated rats

Pro-inflammatory cytokines are known to play a critical role in the early phase of an inflammatory response of ALI, and contribute to the severity of lung injury. To further examine the inhibitory effect of **7a** on cytokines production, the levels of pro-inflammatory cytokines and neutrophils were measured in BALF and serum collected from animals. As shown in Fig. 6A–C, cytokine levels were found to be elevated after LPS challenge compared with naive animals. Conversely, administration of **7a** at a dose of 10 or 20 mg/kg, could significantly down-regulate the levels of IL-6 in BALF and serum, as well as TNF- $\alpha$  in BALF on LPS induced ALI rats.

Additionally, compound **7a** was found to significantly decrease the number of total cells in BALF compared to that of the LPS group (Fig. 6D). Myeloperoxidase (MPO) activity was measured as a marker of tissue neutrophil infiltration. The data presented demonstrates that LPS challenge resulted in significant increases in lung neutrophil infiltration compared with the control group, whereas the increase was significantly attenuated under treatment with various dosages of **7a**, suggesting that neutrophil infiltration was suppressed by **7a** (Fig. 6E).

To verify these findings, we further performed immunohistochemistry analysis with CD68, a general macrophage marker, and TNF- $\alpha$ . As shown in Fig. 6F, LPS alone causes a significant accumulation of CD68-immunostained positive macrophage in the lung sections, whereas there was no significant change in the number of CD68-stained macrophages between **7a** pretreatment and control groups. LPS injection also induced the increase of TNF- $\alpha$  expression in lung tissue and administration **7a** attenuated the TNF- $\alpha$  level (Fig. 6G). Our results highly suggested administration of **7a** resulted in a significant therapeutic effect on LPS-induced pulmonary inflammation.

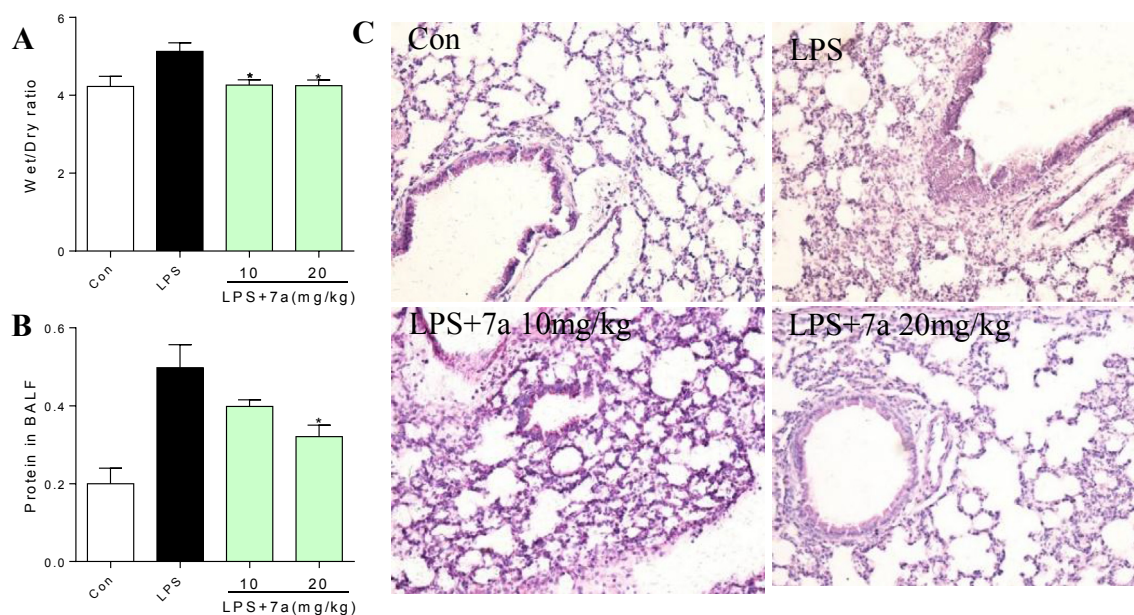


**Fig. 5.** **7a** attenuate the LPS-induced ALI in rats. Rats were intratracheal instillation of LPS. 6 h later, rats were anaesthetized and killed. Bronchoalveolar lavage fluid and lung tissues were collected for further tests. (A) Wet/Dry ratio. (B) Protein concentration in BALF. (C) HE staining.

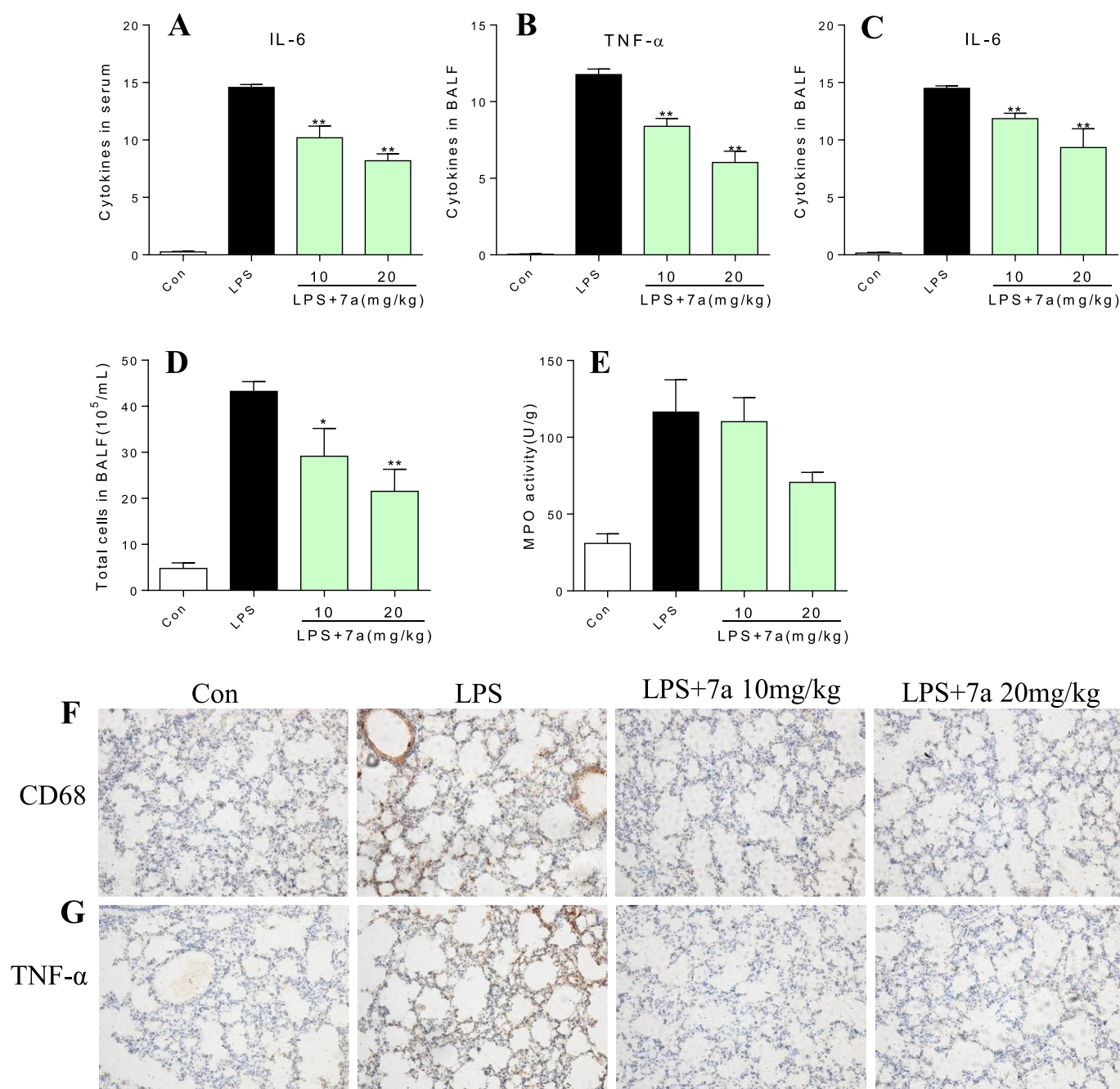


**Fig. 6.** **7a** attenuate the LPS-induced lung inflammation in rats. Rats were intratracheal instillation of LPS. 6 h later, rats were anaesthetized and killed. Bronchoalveolar lavage fluid and lung tissues were collected for further tests. (A) The number of inflammatory cells in BALF. (B) MPO activity. (C) Serum Level of the cytokine IL-6. (D) BALF Level of the cytokine TNF- $\alpha$ . (E) BALF Level of the cytokine IL-6. (F) Immunohistochemical of CD68 staining.

### 3.7. Effects of **7a** on mRNA expression of pro-inflammatory cytokines in Beas-2B cells

We next investigated the effects of **7a** on messenger RNA (mRNA) expression of pro-inflammatory cytokine IL-6, IL-1 $\beta$ , TNF- $\alpha$ , and vascular cell adhesion molecule 1 (VCAM-1) in LPS-stimulated Beas-2B cells. Beas-2B cells were treated with LPS (1.0 mg/mL) for 6 h and examined for the expression of pro-inflammatory genes with or without the **7a** present using quantitative reverse transcription PCR (RT-qPCR) study. As shown in Fig. 7, LPS significantly induced mRNA expressions of IL-6, IL-1 $\beta$ , TNF- $\alpha$ , and VCAM-1 were observed in LPS-stimulated Beas-2B cells, while

the elevated expressions were inhibited by pretreatment of **7a** in a dose-dependent manner. This further validates that compound **7a** has the potential to be used as an anti-inflammatory agent for ALI treatment.

## 4. Conclusion

To develop a novel and water-soluble anti-inflammatory drug for ALI treatment, we explored a series of allylated MACs bearing a piperidone motif based on **8f**, previously reported, as a lead molecule. Among the prepared derivatives, a portion of them had good water solubility as hydrochloride salts even if their ClogP

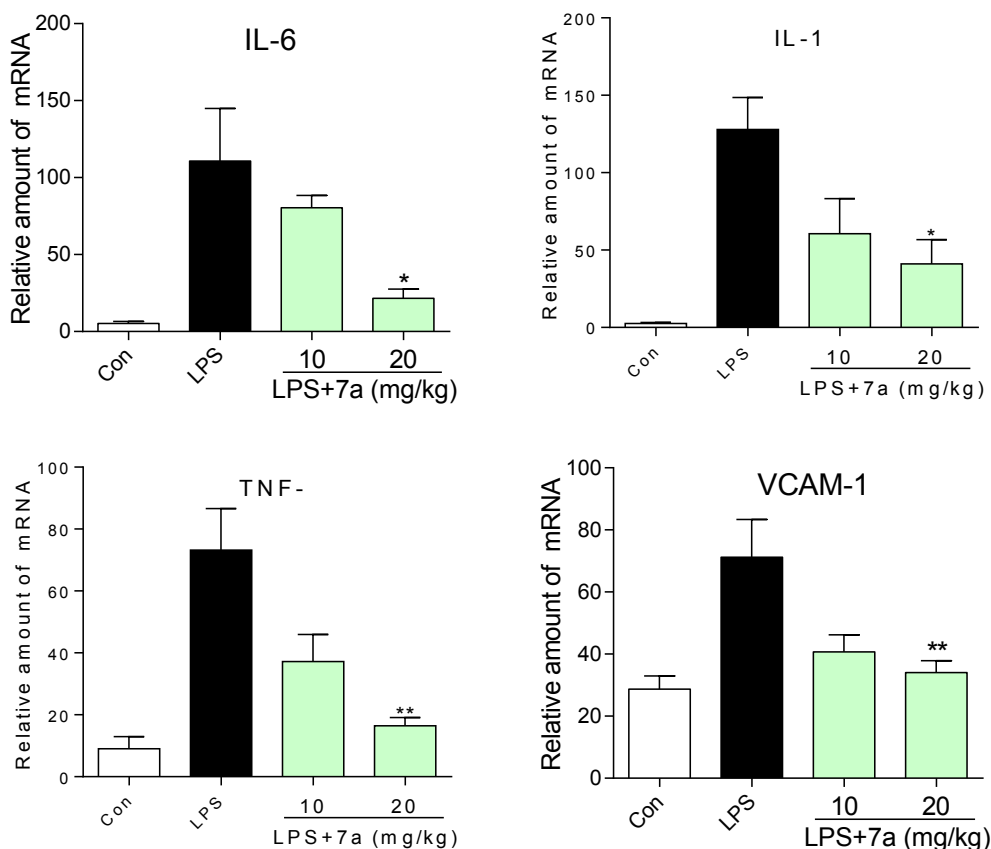


**Fig. 7.** **7a** inhibited the inflammatory genes expression induced by LPS in Beas-2B cells. Cells were plated at a density of  $7.0 \times 10^5$ /plate overnight in  $37^\circ\text{C}$  and  $5\% \text{CO}_2$ . Beas-2B were pretreated with  $10 \mu\text{M}$  **7a** for 30 min and subsequently incubated with LPS ( $1 \mu\text{g}/\text{mL}$ ) for 24 h. Cells were collected and the total RNA was extracted. The mRNA levels of inflammatory cytokines were detected by QPCR (A–D). The results were presented as the percent of LPS control. Each bar represents the mean  $\pm$  SEM of the three independent experiments. Statistical significance relative to the LPS group was indicated, \* $P < 0.05$ ; \*\* $P < 0.01$ .

values were over 4.0. Bioassay results demonstrated that the majority of compounds possessed higher inhibitory activities compared with **8f**, against LPS-induced TNF- $\alpha$  and IL-6 release in RAW 264.7 macrophages. Pretreatment with active compound **7a** results in a significant reduction in the W/D ratio, protein leakage in the BALF, and inflammatory cell infiltration into lung tissue. Histological examination also shows that **7a** has a significant anti-inflammatory activity during LPS-induced ALI. Further, *in vivo* experiment showed that **7a** could attenuate LPS-induced ALI in rats, while effectively inhibiting the expression of IL-6, IL-1 $\beta$ , TNF- $\alpha$ , and VCAM-1 in Beas-2B cells, acting at the mRNA level. Meanwhile, these novel synthetic allylated MACs showed excellent chemical stability *in vitro*, thereby providing a perspective on the possibility of establishing oral drug bioavailability. Taken together, these results may be particularly useful for further pharmaceutical development to treat LPS-induced ALI.

## 5. Experimental section

### 5.1. Chemistry

#### 5.1.1. General

Reagents, solvents, and other chemicals were used as purchased without further purification. All reagents for synthesis were obtained from Sigma Aldrich and Energy-Chemical. Thin-layer chromatography (TLC) was performed on Kiesel-gel 60 F<sub>254</sub> plates and flash column chromatography (medium pressure liquid chromatography) purifications were carried out using Merck silica gel 60

(200–300 mesh ASTM) (Merck KGaA, Darmstadt, Germany). Melting points were determined on a Fisher-Johns melting apparatus and were uncorrected.  $^1\text{H}$  NMR and  $^{13}\text{C}$  NMR spectra were recorded on a Bruker 600 MHz instruments. The chemical shifts were presented in terms of parts per million with TMS as the internal reference. Electrospray ionization mass spectra in positive mode (ESI-MS) data were recorded on a Bruker Esquire 3000t spectrometer, and high-resolution mass spectra ( $m/z$ ) were recorded on a micrOTOF-Q II instrument. All general chemicals were the highest available grade.

#### 5.1.2. Synthesis of 4-(allyloxy)benzaldehyde (**2**)

Allyl bromide (14.0 mL, 163.7 mmol) and  $\text{K}_2\text{CO}_3$  (5.6 g, 40.9 mmol) were added into a solution of 4-hydroxybenzaldehyde (**1**) (10.0 g, 81.9 mmol) in dry acetone (40 mL) and the mixture was stirred overnight at  $65^\circ\text{C}$ . The reaction mixture was concentrated under reduced pressure. The residue was dissolved in EtOAc (30 mL) and washed by water (30 mL), dried over  $\text{MgSO}_4$  and concentrated under reduced pressure. The residue was purified by chromatography on silica gel to give target benzaldehyde **2** (9.96 g, 75%) as a colorless clear liquid.

#### 5.1.3. Synthesis of 3-allyl-4-hydroxybenzaldehyde (**3**)

4-(Allyloxy)benzaldehyde (**2**) (2.3 g, 18.5 mmol) was added into reaction flask, followed by *N,N*-diethylaniline (8.0 mL) dropwise under argon. The reaction mixture was refluxed on a sand bath ( $200^\circ\text{C}$ ) for 5 h. The resulting mixture was cooled down to room temperature, and purified by column chromatography directly

yielded 3-allyl-4-hydroxybenzaldehyde (**3**) (996 mg, 33.2%) as a brown liquid.

#### 5.1.4. General procedure for synthesis of **4a–l**

To a solution of 3-allyl-4-hydroxybenzaldehyde (**3**) (1.0 mmol) in glacial acetic acid (10 mL) added piperidone or different substituted piperidone (0.5 mmol) in glacial acetic acid (4.0 mL). The reaction mixture was stirred for two days at room temperature. The resulting mixture was treated with saturated NaHCO<sub>3</sub> aqueous solution to adjust pH to 7.0, and extracted by EtOAc (3 × 20 mL). The combined organic layers were washed with brine and dried over anhydrous MgSO<sub>4</sub>, filtered, and concentrated under reduced pressure. The residue was further purified by chromatography on silica gel to give the desired symmetric allylated MACs **4a–l**.

**5.1.4.1. (3E,5E)-3,5-Bis(3-allyl-4-hydroxybenzylidene)piperidin-4-one (4a)**. Yellow power. Yield: 25%. m.p.: 196.2–198.3 °C. <sup>1</sup>H NMR (600 MHz, DMSO-*d*<sub>6</sub>) δ (ppm): 9.97 (2H, s, Ar–OH), 7.47 (2H, s, H-β), 7.19 (2H, d, *J* = 8.4 Hz, H-6, H-6'), 7.18 (2H, s, H-2, H-2'), 6.89 (2H, d, *J* = 8.4 Hz, H-5, H-5'), 6.01–5.94 (2H, m, A,B-ArCH<sub>2</sub>CH=CH<sub>2</sub>), 5.08–5.03 (4H, m, A,B-ArCH<sub>2</sub>CH=CH<sub>2</sub>), 3.94 (4H, s, piperidone-CH<sub>2</sub>-N-CH<sub>2</sub>), 3.31 (4H, s, A,B-ArCH<sub>2</sub>CH=CH<sub>2</sub>), 1.99 (1H, s, -NH). <sup>13</sup>C NMR (150 MHz, DMSO-*d*<sub>6</sub>) δ (ppm): 186.9 (-CO-), 156.3 × 2 (C-4, C-4'), 136.8 × 2 (C-β, C-β'), 134.2 × 2 (C-α, C-α'), 132.7 × 2 (A,B-ArCH<sub>2</sub>CH=CH<sub>2</sub>), 132.6 × 2 (C-2, C-2'), 130.4 × 2 (C-3, C-3'), 126.5 × 2 (C-1, C-1'), 126.1 × 2 (C-6, C-6'), 115.6 × 2 (A,B-ArCH<sub>2</sub>CH=CH<sub>2</sub>), 115.2 × 2 (C-5, C-5'), 47.5 × 2 (piperidone-CH<sub>2</sub>-N-CH<sub>2</sub>), 33.6 × 2 (A,B-ArCH<sub>2</sub>CH=CH<sub>2</sub>). ESI-MS, *m/z*: 385.9 (M-H)<sup>-</sup>. HRMS (ESI): calcd for C<sub>25</sub>H<sub>25</sub>NO<sub>3</sub> [M+H]<sup>+</sup>: 388.1907, found: 388.1909.

**5.1.4.2. (3E,5E)-3,5-Bis(3-allyl-4-hydroxybenzylidene)-1-methylpiperidin-4-one (4b)**. Yellow power. Yield: 30%. m.p.: 185.9–187.6 °C. <sup>1</sup>H NMR (600 MHz, DMSO-*d*<sub>6</sub>) δ (ppm): 10.01 (2H, s, Ar–OH), 7.48 (2H, s, H-β, H-β'), 7.21 (2H, d, *J* = 8.4 Hz, H-6, H-6'), 7.20 (2H, s, H-2, H-2'), 6.90 (2H, d, *J* = 8.4 Hz, H-5, H-5'), 6.01–5.94 (2H, m, A,B-ArCH<sub>2</sub>CH=CH<sub>2</sub>), 5.08–5.03 (4H, m, A,B-ArCH<sub>2</sub>CH=CH<sub>2</sub>), 3.67 (4H, s, piperidone-CH<sub>2</sub>-N-CH<sub>2</sub>), 3.31 (4H, s, A,B-ArCH<sub>2</sub>CH=CH<sub>2</sub>), 2.38 (3H, s, N-CH<sub>3</sub>). <sup>13</sup>C NMR (150 MHz, DMSO-*d*<sub>6</sub>) δ (ppm): 185.9 (-CO-), 156.4 × 2 (C-4, C-4'), 136.7 × 2 (C-β, C-β'), 134.8 × 2 (C-α, C-α'), 132.9 × 2 (A,B-ArCH<sub>2</sub>CH=CH<sub>2</sub>), 130.7 × 2 (C-2, C-2'), 130.1 × 2 (C-3, C-3'), 126.5 × 2 (C-1, C-1'), 125.8 × 2 (C-6, C-6'), 115.6 × 2 (A,B-ArCH<sub>2</sub>CH=CH<sub>2</sub>), 115.3 × 2 (C-5, C-5'), 56.6 × 2 (piperidone-CH<sub>2</sub>-N-CH<sub>2</sub>), 45.4 (N-CH<sub>3</sub>), 33.5 × 2 (A,B-ArCH<sub>2</sub>CH=CH<sub>2</sub>). ESI-MS, *m/z*: 400.0 (M-H)<sup>-</sup>. HRMS (ESI): calcd for C<sub>25</sub>H<sub>25</sub>NO<sub>3</sub> [M+H]<sup>+</sup>: 388.1907, found: 388.1909.

**5.1.4.3. (3E,5E)-3,5-Bis(3-allyl-4-hydroxybenzylidene)-1-ethylpiperidin-4-one (4c)**. Yellow power. Yield: 30%. m.p.: 181.3–183.2 °C. <sup>1</sup>H NMR (600 MHz, DMSO-*d*<sub>6</sub>) δ (ppm): 10.01 (2H, s, Ar–OH), 7.49 (2H, s, H-β, H-β'), 7.22 (2H, d, *J* = 8.4 Hz, H-6, H-6'), 7.21 (2H, s, H-2, H-2'), 6.90 (2H, d, *J* = 8.4 Hz, H-5, H-5'), 6.01–5.95 (2H, m, A,B-ArCH<sub>2</sub>CH=CH<sub>2</sub>), 5.08–5.03 (4H, m, A,B-ArCH<sub>2</sub>CH=CH<sub>2</sub>), 3.71 (4H, s, piperidone-CH<sub>2</sub>-N-CH<sub>2</sub>), 3.32 (4H, d, *J* = 6.6 Hz, A,B-ArCH<sub>2</sub>CH=CH<sub>2</sub>), 2.56 (2H, q, *J* = 7.2 Hz, N-CH<sub>2</sub>CH<sub>3</sub>), 0.99 (3H, t, *J* = 7.2 Hz, N-CH<sub>2</sub>CH<sub>3</sub>). <sup>13</sup>C NMR (150 MHz, DMSO-*d*<sub>6</sub>) δ (ppm): 186.3 (-CO-), 156.4 × 2 (C-4, C-4'), 136.8 × 2 (C-β, C-β'), 134.8 × 2 (C-α, C-α'), 132.7 × 2 (A,B-ArCH<sub>2</sub>CH=CH<sub>2</sub>), 130.8 × 2 (C-2, C-2'), 130.3 × 2 (C-3, C-3'), 126.5 × 2 (C-1, C-1'), 125.9 × 2 (C-6, C-6'), 115.7 × 2 (A,B-ArCH<sub>2</sub>CH=CH<sub>2</sub>), 115.3 × 2 (C-5, C-5'), 53.9 × 2 (piperidone-CH<sub>2</sub>-N-CH<sub>2</sub>), 50.7 (N-CH<sub>2</sub>CH<sub>3</sub>), 33.5 × 2 (A,B-ArCH<sub>2</sub>CH=CH<sub>2</sub>), 12.10 (N-CH<sub>2</sub>CH<sub>3</sub>). ESI-MS, *m/z*: 414.1 (M-H)<sup>-</sup>. HRMS (ESI): calcd for C<sub>27</sub>H<sub>29</sub>NO<sub>3</sub> [M+H]<sup>+</sup>: 416.2220, found: 416.2246.

**5.1.4.4. (3E,5E)-3,5-Bis(3-allyl-4-hydroxybenzylidene)-1-propylpiperidin-4-one (4d)**. Yellow power. Yield: 30%. m.p.: 172.9–175.2 °C. <sup>1</sup>H NMR (600 MHz, DMSO-*d*<sub>6</sub>) δ (ppm): 10.01 (2H, s, Ar–OH), 7.49 (2H, s, H-β, H-β'), 7.26 (2H, d, *J* = 8.4 Hz, H-6, H-6'), 7.20 (2H, s, H-2, H-2'), 6.90 (2H, d, *J* = 8.4 Hz, H-5, H-5'), 6.01–5.95 (2H, m, A,B-ArCH<sub>2</sub>CH=CH<sub>2</sub>), 5.08–5.03 (4H, m, A,B-ArCH<sub>2</sub>CH=CH<sub>2</sub>), 3.71 (4H, s, piperidone-CH<sub>2</sub>-N-CH<sub>2</sub>), 3.31 (4H, s, A,B-ArCH<sub>2</sub>CH=CH<sub>2</sub>), 2.47 (2H, t, *J* = 7.2 Hz, N-CH<sub>2</sub>CH<sub>2</sub>CH<sub>3</sub>), 1.43–1.37 (2H, m, N-CH<sub>2</sub>CH<sub>2</sub>CH<sub>3</sub>), 0.80 (3H, t, *J* = 7.2 Hz, N-CH<sub>2</sub>CH<sub>2</sub>CH<sub>3</sub>). <sup>13</sup>C NMR (150 MHz, DMSO-*d*<sub>6</sub>) δ (ppm): 186.2 (-CO-), 156.4 × 2 (C-4, C-4'), 136.8 × 2 (C-β, C-β'), 134.9 × 2 (C-α, C-α'), 132.8 × 2 (A,B-ArCH<sub>2</sub>CH=CH<sub>2</sub>), 130.8 × 2 (C-2, C-2'), 130.3 × 2 (C-3, C-3'), 126.5 × 2 (C-1, C-1'), 125.9 × 2 (C-6, C-6'), 115.6 × 2 (A,B-ArCH<sub>2</sub>CH=CH<sub>2</sub>), 115.3 × 2 (C-5, C-5'), 58.6 (N-CH<sub>2</sub>CH<sub>2</sub>CH<sub>3</sub>), 54.4 × 2 (piperidone-CH<sub>2</sub>-N-CH<sub>2</sub>), 33.5 × 2 (A,B-ArCH<sub>2</sub>CH=CH<sub>2</sub>), 19.8 (N-CH<sub>2</sub>CH<sub>2</sub>CH<sub>3</sub>), 11.7 (N-CH<sub>2</sub>CH<sub>2</sub>CH<sub>3</sub>). ESI-MS, *m/z*: 428.3 (M-H)<sup>-</sup>. HRMS (ESI): calcd for C<sub>28</sub>H<sub>31</sub>NO<sub>3</sub> [M+H]<sup>+</sup>: 430.2377, found: 430.2396.

**5.1.4.5. (3E,5E)-3,5-Bis(3-allyl-4-hydroxybenzylidene)-1-isopropylpiperidin-4-one (4e)**. Yellow power. Yield: 30%. m.p.: 205.3–207.2 °C. <sup>1</sup>H NMR (600 MHz, DMSO-*d*<sub>6</sub>) δ (ppm): 9.99 (2H, s, Ar–OH), 7.47 (2H, s, H-β, H-β'), 7.23 (2H, d, *J* = 7.8 Hz, H-6, H-6'), 7.21 (2H, s, H-2, H-2'), 6.90 (2H, d, *J* = 7.8 Hz, H-5, H-5'), 6.02–5.95 (2H, m, A,B-ArCH<sub>2</sub>CH=CH<sub>2</sub>), 5.09–5.04 (4H, m, A,B-ArCH<sub>2</sub>CH=CH<sub>2</sub>), 3.75 (4H, s, piperidone-CH<sub>2</sub>-N-CH<sub>2</sub>), 3.31 (4H, s, A,B-ArCH<sub>2</sub>CH=CH<sub>2</sub>), 2.91–2.87 (1H, m, N-CH(CH<sub>3</sub>)<sub>2</sub>), 1.02 (6H, d, *J* = 6.6 Hz, N-CH(CH<sub>3</sub>)<sub>2</sub>). <sup>13</sup>C NMR (150 MHz, DMSO-*d*<sub>6</sub>) δ (ppm): 186.7 (-CO-), 156.3 × 2 (C-4, C-4'), 136.8 × 2 (C-β, C-β'), 134.3 × 2 (C-α, C-α'), 132.6 × 2 (A,B-ArCH<sub>2</sub>CH=CH<sub>2</sub>), 131.5 × 2 (C-2, C-2'), 130.3 × 2 (C-3, C-3'), 126.5 × 2 (C-1, C-1'), 125.9 × 2 (C-6, C-6'), 115.7 × 2 (A,B-ArCH<sub>2</sub>CH=CH<sub>2</sub>), 115.3 × 2 (C-5, C-5'), 53.1 (N-CH(CH<sub>3</sub>)<sub>2</sub>), 50.1 × 2 (piperidone-CH<sub>2</sub>-N-CH<sub>2</sub>), 33.4 × 2 (A,B-ArCH<sub>2</sub>CH=CH<sub>2</sub>), 18.1 × 2 (N-CH(CH<sub>3</sub>)<sub>2</sub>). ESI-MS, *m/z*: 428.1 (M-H)<sup>-</sup>. HRMS (ESI): calcd for C<sub>28</sub>H<sub>31</sub>NO<sub>3</sub> [M+H]<sup>+</sup>: 430.2377, found: 430.2396.

**5.1.4.6. (3E,5E)-3,5-Bis(3-allyl-4-hydroxybenzylidene)-1-cyclopropylpiperidin-4-one (4f)**. Yellow power. Yield: 40%. m.p.: 82.5–85.1 °C. <sup>1</sup>H NMR (600 MHz, DMSO-*d*<sub>6</sub>) δ (ppm): 10.01 (2H, s, Ar–OH), 7.49 (2H, s, H-β, H-β'), 7.22 (2H, d, *J* = 8.4 Hz, H-6, H-6'), 7.21 (2H, s, H-2, H-2'), 6.92 (2H, d, *J* = 8.4 Hz, H-5, H-5'), 6.02–5.95 (2H, m, A,B-ArCH<sub>2</sub>CH=CH<sub>2</sub>), 5.08–5.04 (4H, m, A,B-ArCH<sub>2</sub>CH=CH<sub>2</sub>), 3.89 (4H, s, piperidone-CH<sub>2</sub>-N-CH<sub>2</sub>), 3.31 (4H, s, A,B-ArCH<sub>2</sub>CH=CH<sub>2</sub>), 1.99–1.96 (1H, m, N-CH-Cyclopropyl), 0.47–0.44 (2H, m, N-CH<sub>2</sub>-Cyclopropyl), 0.28–0.25 (2H, m, N-CH<sub>2</sub>-Cyclopropyl). <sup>13</sup>C NMR (150 MHz, DMSO-*d*<sub>6</sub>) δ (ppm): 186.1 (-CO-), 156.4 × 2 (C-4, C-4'), 136.7 × 2 (C-β, C-β'), 134.9 × 2 (C-α, C-α'), 132.9 × 2 (A,B-ArCH<sub>2</sub>CH=CH<sub>2</sub>), 130.8 × 2 (C-2, C-2'), 130.1 × 2 (C-3, C-3'), 126.6 × 2 (C-1, C-1'), 125.9 × 2 (C-6, C-6'), 115.7 × 2 (A,B-ArCH<sub>2</sub>CH=CH<sub>2</sub>), 115.3 × 2 (C-5, C-5'), 54.5 × 2 (piperidone-CH<sub>2</sub>-N-CH<sub>2</sub>), 37.5 (N-CH-Cyclopropyl), 33.5 × 2 (A,B-ArCH<sub>2</sub>CH=CH<sub>2</sub>), 6.4 × 2 (N-CH<sub>2</sub>-Cyclopropyl). ESI-MS, *m/z*: 426.1 (M-H)<sup>-</sup>. HRMS (ESI): calcd for C<sub>28</sub>H<sub>29</sub>NO<sub>3</sub> [M+H]<sup>+</sup>: 428.2220, found: 428.2229.

**5.1.4.7. (3E,5E)-3,5-Bis(3-allyl-4-hydroxybenzylidene)-1-(phenylsulfonyl)piperidin-4-one (4g)**. Yellow power. Yield: 35%. m.p.: 84.7–87.0 °C. <sup>1</sup>H NMR (600 MHz, DMSO-*d*<sub>6</sub>) δ (ppm): 10.18 (2H, s, Ar–OH), 7.74–7.71 (1H, m, -N-SO<sub>2</sub>-Ar-H-4), 7.60–7.59 (4H, m, N-SO<sub>4</sub>-Ar-H-2,3,5,6), 7.48 (2H, s, H-β, H-β'), 7.22 (2H, dd, *J*<sub>1</sub> = 8.4 Hz, *J*<sub>2</sub> = 1.8 Hz, H-6, H-6'), 7.14 (2H, s, H-2, H-2'), 6.95 (2H, d, *J* = 8.4 Hz, H-5, H-5'), 6.05–5.98 (2H, m, A,B-ArCH<sub>2</sub>CH=CH<sub>2</sub>), 5.14–5.08 (4H, m, A,B-ArCH<sub>2</sub>CH=CH<sub>2</sub>), 4.49 (4H, s, piperidone-CH<sub>2</sub>-N-CH<sub>2</sub>), 3.35 (4H, s, A,B-ArCH<sub>2</sub>CH=CH<sub>2</sub>). <sup>13</sup>C NMR

(150 MHz, DMSO-*d*<sub>6</sub>)  $\delta$  (ppm): 183.7 ( $-\text{CO}-$ ), 156.9  $\times$  2 (C-4, C-4'), 137.3  $\times$  2 (C- $\beta$ , C- $\beta'$ ), 136.8 (N-SO<sub>4</sub>-Ar-C-1), 136.7  $\times$  2 (C- $\alpha$ , C- $\alpha'$ ), 133.6 (N-SO<sub>4</sub>-Ar-C-4), 132.6  $\times$  2 (A,B-ArCH<sub>2</sub>CH=CH<sub>2</sub>), 130.6  $\times$  2 (C-2, C-2'), 129.5  $\times$  2 (C-3, C-3'), 127.5  $\times$  2 (N-SO<sub>4</sub>-Ar-C-3.5), 127.2  $\times$  2 (C-1, C-1'), 126.8  $\times$  2 (C-6, C-6'), 125.2  $\times$  2 (N-SO<sub>4</sub>-Ar-C-2.6), 115.9  $\times$  2 (A,B-ArCH<sub>2</sub>CH=CH<sub>2</sub>), 115.5  $\times$  2 (C-5, C-5'), 56.1  $\times$  2 (piperidone-CH<sub>2</sub>-N-CH<sub>2</sub>), 33.5  $\times$  2 (A,B-ArCH<sub>2</sub>CH=CH<sub>2</sub>). ESI-MS, *m/z*: 526.3 (M-H)<sup>-</sup>. HRMS (ESI): calcd for C<sub>31</sub>H<sub>29</sub>NO<sub>5</sub>S [M+H]<sup>+</sup>: 528.1839, found: 528.1844.

**5.1.4.8. (3E,5E)-3,5-Bis(3-allyl-4-hydroxybenzylidene)-1-benzylpiperidin-4-one (4h).** Yellow powder. Yield: 35%. m.p: 135.9–137.8 °C. <sup>1</sup>H NMR (600 MHz, DMSO-*d*<sub>6</sub>)  $\delta$  (ppm): 10.16 (2H, s, Ar-OH), 7.74–7.72 (1H, m, N-CH<sub>2</sub>-Benzene-4), 7.60–7.59 (4H, m, N-CH<sub>2</sub>-Benzene-2,3,5,6), 7.48 (2H, s, H- $\beta$ , H- $\beta'$ ), 7.22 (2H, dd, *J*<sub>1</sub> = 8.4 Hz, *J*<sub>2</sub> = 1.8 Hz, H-6, H-6'), 7.15 (2H, s, H-2, H-2'), 6.95 (2H, d, *J* = 8.4 Hz, H-5, H-5'), 6.05–5.98 (2H, m, A,B-ArCH<sub>2</sub>CH=CH<sub>2</sub>), 5.13–5.08 (4H, m, A,B-ArCH<sub>2</sub>CH=CH<sub>2</sub>), 4.50 (4H, s, piperidone-CH<sub>2</sub>-N-CH<sub>2</sub>), 3.36 (2H, s, N-CH<sub>2</sub>-Benzene), 3.35 (4H, s, A,B-ArCH<sub>2</sub>CH=CH<sub>2</sub>). <sup>13</sup>C NMR (150 MHz, DMSO-*d*<sub>6</sub>)  $\delta$  (ppm): 186.1 ( $-\text{CO}-$ ), 156.4  $\times$  2 (C-4, C-4'), 136.6  $\times$  2 (C- $\beta$ , C- $\beta'$ ), 134.9  $\times$  2 (C- $\alpha$ , C- $\alpha'$ ), 132.4  $\times$  2 (A,B-ArCH<sub>2</sub>CH=CH<sub>2</sub>), 130.6  $\times$  2 (C-2, C-2'), 130.5  $\times$  2 (C-3, C-3'), 129.1  $\times$  2 (N-CH<sub>2</sub>-Benzene-C-2.6), 128.7 (N-CH<sub>2</sub>-Benzene-C-1), 128.2  $\times$  2 (N-CH<sub>2</sub>-Benzene-C-3.5), 127.2 (N-CH<sub>2</sub>-Benzene-C-4), 126.5  $\times$  2 (C-1, C-1'), 125.8  $\times$  2 (C-6, C-6'), 115.8  $\times$  2 (A,B-ArCH<sub>2</sub>CH=CH<sub>2</sub>), 115.3  $\times$  2 (C-5, C-5'), 61.2 (N-CH<sub>2</sub>-Benzene), 54.3  $\times$  2 (piperidone-CH<sub>2</sub>-N-CH<sub>2</sub>), 33.5  $\times$  2 (A,B-ArCH<sub>2</sub>CH=CH<sub>2</sub>). ESI-MS, *m/z*: 476.0 (M-H)<sup>-</sup>. HRMS (ESI): calcd for C<sub>32</sub>H<sub>31</sub>NO<sub>3</sub> [M+H]<sup>+</sup>: 478.2377, found: 478.2398.

**5.1.4.9. (3E,5E)-3,5-Bis(3-allyl-4-hydroxybenzylidene)-1-(2,6-dichlorobenzoyl)piperidin-4-one (4i).** Yellow powder. Yield: 34%. m.p: 212.5–214.3 °C. <sup>1</sup>H NMR (600 MHz, DMSO-*d*<sub>6</sub>)  $\delta$  (ppm): 10.17 (2H, s, Ar-OH), 7.58–7.55 (1H, m, -N-CO-Ar-H-4), 7.30 (2H, d, *J* = 7.8 Hz, N-CO-Ar-H-3.5), 7.50 (2H, s, H- $\beta$ , H- $\beta'$ ), 7.36 (2H, d, *J* = 7.8 Hz, H-6, H-6'), 7.24 (2H, d, *J* = 7.8 Hz, H-5, H-5'), 6.97 (2H, s, H-2, H-2'), 6.04–5.97 (2H, m, A,B-ArCH<sub>2</sub>CH=CH<sub>2</sub>), 5.10–5.06 (4H, m, A,B-ArCH<sub>2</sub>CH=CH<sub>2</sub>), 4.49 (4H, s, piperidone-CH<sub>2</sub>-N-CH<sub>2</sub>), 3.31 (4H, s, A,B-ArCH<sub>2</sub>CH=CH<sub>2</sub>). <sup>13</sup>C NMR (150 MHz, DMSO-*d*<sub>6</sub>)  $\delta$  (ppm): 184.8 ( $-\text{CO}-$ ), 162.7 (N-CO-Ar), 156.5  $\times$  2 (C-4, C-4'), 137.23  $\times$  2 (C- $\beta$ , C- $\beta'$ ), 136.7  $\times$  2 (C- $\alpha$ , C- $\alpha'$ ), 133.5 (N-CO-Ar-C-1), 133.3  $\times$  2 (A,B-ArCH<sub>2</sub>CH=CH<sub>2</sub>), 130.4  $\times$  2 (N-CO-Ar-C-2.6), 128.1  $\times$  3 (C-2, C-2', N-CO-Ar-C-4), 126.8  $\times$  2 (C-3, C-3'), 126.3  $\times$  2 (N-CO-Ar-C-3.5), 125.4  $\times$  2 (C-1, C-1'), 125.0  $\times$  2 (C-6, C-6'), 115.9  $\times$  2 (A,B-ArCH<sub>2</sub>CH=CH<sub>2</sub>), 115.7  $\times$  2 (C-5, C-5'), 46.3  $\times$  2 (piperidone-CH<sub>2</sub>-N-CH<sub>2</sub>), 33.6  $\times$  2 (A,B-ArCH<sub>2</sub>CH=CH<sub>2</sub>). ESI-MS, *m/z*: 558.2 (M-H)<sup>-</sup>. HRMS (ESI): calcd for C<sub>32</sub>H<sub>27</sub>Cl<sub>2</sub>NO<sub>4</sub> [M+H]<sup>+</sup>: 560.1390, found: 560.1407.

**5.1.4.10. (3E,5E)-3,5-Bis(3-allyl-4-hydroxybenzylidene)-1-(4-fluorobenzoyl)piperidin-4-one (4j).** Yellow powder. Yield: 30%. m.p: 210.3–212.1 °C. <sup>1</sup>H NMR (600 MHz, DMSO-*d*<sub>6</sub>)  $\delta$  (ppm): 10.11 (2H, s, Ar-OH), 7.74 (2H, d, *J* = 9.0 Hz, -N-CO-Ar-H-2.6), 7.68 (2H, d, *J* = 9.0 Hz, N-CO-Ar-H-3.5), 7.63 (2H, s, H- $\beta$ , H- $\beta'$ ), 7.56 (2H, d, *J* = 8.4 Hz, H-6, H-6'), 7.27 (2H, d, *J* = 8.4 Hz, H-5, H-5'), 6.98 (2H, s, H-2, H-2'), 5.99–5.94 (2H, m, A,B-ArCH<sub>2</sub>CH=CH<sub>2</sub>), 5.01–4.95 (4H, m, A,B-ArCH<sub>2</sub>CH=CH<sub>2</sub>), 4.02 (4H, s, piperidone-CH<sub>2</sub>-N-CH<sub>2</sub>), 3.30 (4H, s, A,B-ArCH<sub>2</sub>CH=CH<sub>2</sub>). <sup>13</sup>C NMR (150 MHz, DMSO-*d*<sub>6</sub>)  $\delta$  (ppm): 185.2 ( $-\text{CO}-$ ), 168.6 (N-CO-Ar), 166.9 (N-CO-Ar-C-4), 156.6  $\times$  2 (C-4, C-4'), 136.6  $\times$  2 (C- $\beta$ , C- $\beta'$ ), 136.5  $\times$  2 (C- $\alpha$ , C- $\alpha'$ ), 131.7  $\times$  2 (A,B-ArCH<sub>2</sub>CH=CH<sub>2</sub>), 131.5  $\times$  2 (C-2, C-2'), 129.5 (N-CO-Ar-C-1), 129.4  $\times$  2 (C-3, C-3'), 129.3  $\times$  2 (N-CO-Ar-C-2.6), 129.2  $\times$  2 (C-1, C-1'), 128.7  $\times$  2 (C-6, C-6'), 115.5  $\times$  2 (A,B-ArCH<sub>2</sub>CH=CH<sub>2</sub>), 115.3  $\times$  2 (C-5, C-5'), 115.1  $\times$  2 (N-CO-Ar-C-3.5), 46.4  $\times$  2 (piperidone-CH<sub>2</sub>-N-CH<sub>2</sub>), 33.5  $\times$  2 (A,B-ArCH<sub>2</sub>CH=CH<sub>2</sub>). ESI-MS, *m/z*: 508.1 (M-H)<sup>-</sup>. HRMS (ESI): calcd for C<sub>32</sub>H<sub>28</sub>FNO<sub>4</sub> [M+H]<sup>+</sup>:

510.2075, found: 510.2090.

**5.1.4.11. (3E,5E)-3,5-Bis(3-allyl-4-hydroxybenzylidene)-1-(4-chlorobenzoyl)piperidin-4-one (4k).** Yellow powder. Yield: 30%. m.p: 217.6–220.0 °C. <sup>1</sup>H NMR (600 MHz, DMSO-*d*<sub>6</sub>)  $\delta$  (ppm): 10.13 (2H, s, Ar-OH), 7.74 (2H, d, *J* = 9.0 Hz, -N-CO-Ar-H-2.6), 7.67 (2H, d, *J* = 9.0 Hz, N-CO-Ar-H-3.5), 7.61 (2H, s, H- $\beta$ , H- $\beta'$ ), 7.52 (2H, d, *J* = 8.4 Hz, H-6, H-6'), 7.22 (2H, d, *J* = 8.4 Hz, H-5, H-5'), 6.97 (2H, s, H-2, H-2'), 5.99–5.94 (2H, m, A,B-ArCH<sub>2</sub>CH=CH<sub>2</sub>), 5.06–5.02 (4H, m, A,B-ArCH<sub>2</sub>CH=CH<sub>2</sub>), 4.02 (4H, s, piperidone-CH<sub>2</sub>-N-CH<sub>2</sub>), 3.31 (4H, s, A,B-ArCH<sub>2</sub>CH=CH<sub>2</sub>). <sup>13</sup>C NMR (150 MHz, DMSO-*d*<sub>6</sub>)  $\delta$  (ppm): 185.2 ( $-\text{CO}-$ ), 168.5 (N-CO-Ar), 156.9  $\times$  2 (C-4, C-4'), 136.6  $\times$  2 (C- $\beta$ , C- $\beta'$ ), 134.4 (N-CO-Ar-C-4), 133.4 (N-CO-Ar-C-1), 131.7  $\times$  2 (C- $\alpha$ , C- $\alpha'$ ), 131.5  $\times$  2 (A,B-ArCH<sub>2</sub>CH=CH<sub>2</sub>), 130.6  $\times$  2 (C-2, C-2'), 128.8  $\times$  2 (N-CO-Ar-C-2.6), 128.7  $\times$  2 (C-3, C-3'), 128.5  $\times$  2 (N-CO-Ar-C-3.5), 128.4  $\times$  2 (C-1, C-1'), 128.2  $\times$  2 (C-6, C-6'), 115.5  $\times$  2 (A,B-ArCH<sub>2</sub>CH=CH<sub>2</sub>), 115.4  $\times$  2 (C-5, C-5'), 54.9  $\times$  2 (piperidone-CH<sub>2</sub>-N-CH<sub>2</sub>), 33.5  $\times$  2 (A,B-ArCH<sub>2</sub>CH=CH<sub>2</sub>). ESI-MS, *m/z*: 524.1 (M-H)<sup>-</sup>. HRMS (ESI): calcd for C<sub>32</sub>H<sub>28</sub>ClNO<sub>4</sub> [M+H]<sup>+</sup>: 526.1780, found: 526.1783.

**5.1.4.12. (3E,5E)-3,5-Bis(3-allyl-4-hydroxybenzylidene)-1-(4-methylbenzoyl)piperidin-4-one (4l).** Yellow powder. Yield: 25%. m.p: 215.3–217.2 °C. <sup>1</sup>H NMR (600 MHz, DMSO-*d*<sub>6</sub>)  $\delta$  (ppm): 10.11 (2H, s, Ar-OH), 7.63 (2H, d, *J* = 7.8 Hz, -N-CO-Ar-H-2.6), 7.61 (2H, s, H- $\beta$ , H- $\beta'$ ), 7.37 (2H, d, *J* = 7.8 Hz, N-CO-Ar-H-3.5), 7.27 (2H, d, *J* = 8.4 Hz, H-6, H-6'), 7.09 (2H, d, *J* = 8.4 Hz, H-5, H-5'), 6.95 (2H, s, H-2, H-2'), 6.01–5.93 (2H, m, A,B-ArCH<sub>2</sub>CH=CH<sub>2</sub>), 5.09–5.02 (4H, m, A,B-ArCH<sub>2</sub>CH=CH<sub>2</sub>), 4.68 (4H, s, piperidone-CH<sub>2</sub>-N-CH<sub>2</sub>), 3.35 (4H, s, A,B-ArCH<sub>2</sub>CH=CH<sub>2</sub>), 2.34 (3H, s, -CH<sub>3</sub>). <sup>13</sup>C NMR (150 MHz, DMSO-*d*<sub>6</sub>)  $\delta$  (ppm): 185.3 ( $-\text{CO}-$ ), 169.1 (N-CO-Ar), 156.9  $\times$  2 (C-4, C-4'), 139.4  $\times$  2 (C- $\beta$ , C- $\beta'$ ), 136.6  $\times$  2 (C- $\alpha$ , C- $\alpha'$ ), 131.7 (N-CO-Ar-C-4), 130.5  $\times$  2 (A,B-ArCH<sub>2</sub>CH=CH<sub>2</sub>), 129.6 (N-CO-Ar-C-1), 129.4  $\times$  2 (C-2, C-2'), 128.9  $\times$  2 (C-3, C-3'), 128.6  $\times$  2 (N-CO-Ar-C-3.5), 126.9  $\times$  2 (C-1, C-1'), 126.9  $\times$  2 (C-6, C-6'), 126.6  $\times$  2 (N-CO-Ar-C-2.6), 115.7  $\times$  2 (A,B-ArCH<sub>2</sub>CH=CH<sub>2</sub>), 115.3  $\times$  2 (C-5, C-5'), 56.0  $\times$  2 (piperidone-CH<sub>2</sub>-N-CH<sub>2</sub>), 33.5  $\times$  2 (A,B-ArCH<sub>2</sub>CH=CH<sub>2</sub>), 20.8 (N-CO-Ar-CH<sub>3</sub>). ESI-MS, *m/z*: 504.1 (M-H)<sup>-</sup>. HRMS (ESI): calcd for C<sub>33</sub>H<sub>31</sub>NO<sub>4</sub> [M+H]<sup>+</sup>: 506.2326, found: 506.2338.

#### 5.1.5. Synthesis of O-THP protected benzaldehyde (5)

A solution of 3-allyl-4-hydroxybenzaldehyde (**3**) (1.0 g, 6.17 mmol) in dry CH<sub>2</sub>Cl<sub>2</sub> (10 mL) was added 3,4-dihydro-2H-pyran (2.59 g, 30.83 mmol) portionwise, followed by PPTS (200 mg, 0.617 mmol). The reaction mixture was stirred overnight at 40 °C. The resulting solution was quenched with redistilled water (40 mL) and extracted with EtOAc (3  $\times$  50 mL). The combined organic layers were washed with water (100 mL), brine (100 mL), dried over anhydrous MgSO<sub>4</sub>, filtered, and concentrated in vacuo. The residue was purified by chromatography on silica gel provided O-THP protected benzaldehyde **5** (1.29 g, 85%) as a yellow liquid.

#### 5.1.6. Synthesis of $\alpha,\beta$ -unsaturated ketone (6)

To a solution of O-THP protected benzaldehyde (**5**) (500 mg, 2.03 mmol) in CH<sub>2</sub>Cl<sub>2</sub> added 1-cyclopropylpiperidin-4-one (310.83 mg, 2.33 mmol) and pyrrolidine (433.13 mg, 6.09 mmol). The reaction flask was allowed to warm up to 40 °C for 4 h. The resulting mixture was concentrated under reduced pressure, and the residue was purified by silica gel directly to afford the  $\alpha,\beta$ -unsaturated ketone **6** (5.26 g, 40%) as a brown liquid.

#### 5.1.7. General routes for synthesis of 7a-e

To a stirring solution of intermediate (**6**) (0.544 mmol) in EtOH (10 mL) and different substituted benzaldehydes (0.544 mmol) at room temperature was added dropwise a solution of 20% (w/v)

NaOH aqueous solution (0.8 mL). The reaction mixture was stirred overnight at room temperature and the resulting mixture was diluted with saturated sodium bicarbonate aqueous solution (10 mL) and extracted with EtOAc (3 × 20 mL). The combined organic layers were washed with brine (40 mL) and dried over anhydrous MgSO<sub>4</sub>, filtered, and concentrated under reduced pressure. The residue was further dissolved in dry MeOH (5 mL) and dropwise 10 drops of concentrated HCl. The reaction mixture was stirred at room temperature for 5 h, then quenched with saturated aqueous NH<sub>4</sub>Cl solution (5 mL) and extracted with EtOAc (3 × 10 mL). The combined organic layers were washed with brine (15 mL) and dried over anhydrous MgSO<sub>4</sub>, filtered, and concentrated under reduced pressure. The residue was purified by chromatography on silica gel to furnish target asymmetric allylated MACs **7a–e**.

5.1.7.1. (3*E*,5*E*)-3-(3-Allyl-4-hydroxybenzylidene)-1-cyclopropyl-5-[4-(4-methylpiperazin-1-yl)benzylidene]piperidin-4-one (**7a**).

Yellow power. Yield: 20%. m.p.: 210.3–213.1 °C. <sup>1</sup>H NMR (600 MHz, DMSO-*d*<sub>6</sub>) δ (ppm): 7.48 (2H, s, H-β', H-β), 7.35 (2H, d, *J* = 9.0 Hz, H-6', H-2'), 7.16 (1H, d, *J* = 7.2 Hz, H-6), 7.15 (1H, s, H-2), 7.01 (2H, d, *J* = 9.0 Hz, H-5', H-3'), 6.77 (1H, d, *J* = 7.2 Hz, H-5), 6.03–5.96 (1H, m, A-ArCH<sub>2</sub>CH=CH<sub>2</sub>), 5.09–5.02 (2H, m, A-ArCH<sub>2</sub>CH=CH<sub>2</sub>), 3.89 (2H, s, piperidone-CH<sub>2</sub>-N-CH<sub>2</sub>), 3.88 (2H, s, piperidone-CH<sub>2</sub>-N-CH<sub>2</sub>), 3.30 (2H, d, *J* = 6.6 Hz, A-ArCH<sub>2</sub>CH=CH<sub>2</sub>), 3.26 (4H, t, *J* = 4.2 Hz, piperazinyl-N-(CH<sub>2</sub>CH<sub>2</sub>)<sub>2</sub>-N-CH<sub>3</sub>), 2.43 (4H, t, *J* = 4.2 Hz, piperazinyl-N-(CH<sub>2</sub>CH<sub>2</sub>)<sub>2</sub>-N-CH<sub>3</sub>), 2.22 (3H, s, -N-CH<sub>3</sub>), 1.98 (1H, s, -NH-Cyclopropyl(CH<sub>2</sub>-CH<sub>2</sub>)), 0.46 (2H, s, Cyclopropyl(CH<sub>2</sub>-CH<sub>2</sub>)), 0.27 (2H, s, N-CH<sub>2</sub>-CH<sub>2</sub>-Cyclopropyl). <sup>13</sup>C NMR (150 MHz, DMSO-*d*<sub>6</sub>) δ (ppm): 185.5 (-CO-), 151.0 (C-4), 137.4 × 2 (C-β, C-β'), 135.8 (C-α), 134.3 (C-α'), 132.9 (C-8), 132.0 × 4 (C-2', 4', 6', C-2), 130.7 (C-3), 130.6 (C-1), 127.3 (C-6), 124.651 (C-1'), 116.2 (C-9), 115.3 (C-5), 114.3 × 2 (C-3', C-5'), 56.0 × 2 (piperazinyl-N-(CH<sub>2</sub>CH<sub>2</sub>)<sub>2</sub>-N-CH<sub>3</sub>), 54.4 × 2 (piperazinyl-N-(CH<sub>2</sub>CH<sub>2</sub>)<sub>2</sub>-N-CH<sub>3</sub>), 46.9 × 2 (piperidone-CH<sub>2</sub>-N-CH<sub>2</sub>), 45.7 (N-CH<sub>3</sub>), 37.7 (N-CH-Cyclopropyl), 33.9 (C-7), 6.4 × 2 (Cyclopropyl(CH<sub>2</sub>-CH<sub>2</sub>)). ESI-MS, *m/z*: 470.4 (M+H)<sup>+</sup>. HRMS (ESI): calcd for C<sub>30</sub>H<sub>35</sub>N<sub>3</sub>O<sub>2</sub> [M+H]<sup>+</sup>: 470.2802, found: 470.2825.

5.1.7.2. (3*E*,5*E*)-3-(3-Allyl-4-hydroxybenzylidene)-1-cyclopropyl-5-(4-morpholinobenzylidene) piperidin-4-one (**7b**).

Yellow power. Yield: 28%. m.p.: 196.5–198.7 °C. <sup>1</sup>H NMR (600 MHz, DMSO-*d*<sub>6</sub>) δ (ppm): 10.01 (1H, s, Ar-OH), 7.51 (1H, s, H-β'), 7.49 (1H, s, H-β), 7.39 (2H, d, *J* = 9.0 Hz, H-6', H-2'), 7.22 (1H, d, *J* = 7.8 Hz, H-6), 7.21 (1H, s, H-2), 7.03 (2H, d, *J* = 9.0 Hz, H-5', H-3'), 6.92 (1H, d, *J* = 7.8 Hz, H-5), 6.02–5.95 (1H, m, A-ArCH<sub>2</sub>CH=CH<sub>2</sub>), 5.09–5.04 (2H, m, A-ArCH<sub>2</sub>CH=CH<sub>2</sub>), 3.93 (2H, s, piperidone-CH<sub>2</sub>-N-CH<sub>2</sub>), 3.90 (2H, s, piperidone-CH<sub>2</sub>-N-CH<sub>2</sub>), 3.74 (4H, t, *J* = 4.8 Hz, morpholinyl-N-(CH<sub>2</sub>CH<sub>2</sub>)<sub>2</sub>-O), 3.28 (2H, d, *J* = 6.6 Hz, A-ArCH<sub>2</sub>CH=CH<sub>2</sub>), 3.24 (4H, t, *J* = 4.8 Hz, morpholinyl-N-(CH<sub>2</sub>CH<sub>2</sub>)<sub>2</sub>-O), 1.98 (1H, s, -N-CH-Cyclopropyl(CH<sub>2</sub>-CH<sub>2</sub>)), 0.47 (2H, s, -N-CH-Cyclopropyl(CH<sub>2</sub>-CH<sub>2</sub>)), 0.28 (2H, s, -N-CH-Cyclopropyl(CH<sub>2</sub>-CH<sub>2</sub>)). <sup>13</sup>C NMR (150 MHz, DMSO-*d*<sub>6</sub>) δ (ppm): 186.0 (-CO-), 156.4 (C-4), 151.3 (C-4'), 136.7 (C-β), 134.9 (C-β'), 134.8 (C-α), 132.9 (C-α'), 132.1 × 2 (C-2', 6'), 130.9 (C-8), 130.4 (C-2), 130.1 (C-3), 126.6 (C-1), 125.9 (C-6), 124.9 (C-1'), 115.7 (C-9), 115.3 (C-5), 114.2 × 2 (C-3', C-5'), 65.9 × 2 (morpholinyl-N-(CH<sub>2</sub>CH<sub>2</sub>)<sub>2</sub>-O), 54.8 (morpholinyl-N-(CH<sub>2</sub>CH<sub>2</sub>)<sub>2</sub>-O), 54.6 (morpholinyl-N-(CH<sub>2</sub>CH<sub>2</sub>)<sub>2</sub>-O), 47.2 × 2 (piperidone-CH<sub>2</sub>-N-CH<sub>2</sub>), 37.6 (N-CH-Cyclopropyl), 33.5 (C-7), 6.4 × 2 (Cyclopropyl(CH<sub>2</sub>-CH<sub>2</sub>)). ESI-MS, *m/z*: 457.3 (M+H)<sup>+</sup>. HRMS (ESI): calcd for C<sub>29</sub>H<sub>32</sub>N<sub>2</sub>O<sub>3</sub> [M+H]<sup>+</sup>: 457.2486, found: 457.2490.

5.1.7.3. (3*E*,5*E*)-3-(3-Allyl-4-hydroxybenzylidene)-1-cyclopropyl-5-[4-(pyrrolidin-1-yl)benzylidene]piperidin-4-one (**7c**). Yellow power. Yield: 25%. m.p.: 186.8–188.5 °C. <sup>1</sup>H NMR (600 MHz, DMSO-*d*<sub>6</sub>) δ (ppm): 7.50 (1H, s, H-β'), 7.47 (1H, s, H-β), 7.34 (2H, d, *J* = 9.0 Hz, H-6', H-2'), 7.18 (1H, d, *J* = 7.8 Hz, H-6), 7.17 (1H, s, H-2), 6.86 (1H, d, *J* = 8.4 Hz, H-5), 6.63 (2H, d, *J* = 9.0 Hz, H-5', H-3'), 6.02–5.95 (1H, m, A-ArCH<sub>2</sub>CH=CH<sub>2</sub>), 5.08–5.03 (2H, m, A-ArCH<sub>2</sub>CH=CH<sub>2</sub>), 3.90 (2H, s, piperidone-CH<sub>2</sub>-N-CH<sub>2</sub>), 3.88 (2H, s, piperidone-CH<sub>2</sub>-N-CH<sub>2</sub>), 3.30 (2H, d, *J* = 6.6 Hz, A-ArCH<sub>2</sub>CH=CH<sub>2</sub>), 3.29 (4H, t, *J* = 4.8 Hz, pyrrol-N-CH<sub>2</sub>-CH<sub>2</sub>-CH<sub>2</sub>-CH<sub>2</sub>-N), 1.98 (5H, s, -N-CH-Cyclopropyl(CH<sub>2</sub>-CH<sub>2</sub>)), pyrrol-⊖ N-CH<sub>2</sub>-CH<sub>2</sub>-CH<sub>2</sub>-CH<sub>2</sub>-N), 0.47 (2H, s, -N-CH-Cyclopropyl(CH<sub>2</sub>-CH<sub>2</sub>)), 0.27 (2H, s, -N-CH-Cyclopropyl(CH<sub>2</sub>-CH<sub>2</sub>)). <sup>13</sup>C NMR (150 MHz, DMSO-*d*<sub>6</sub>) δ (ppm): 185.6 (-CO-), 148.1 (C-4), 137.0 × 2 (C-β, C-β'), 135.6 (C-4'), 134.7 (C-α), 132.8 × 2 (C-α', C-8), 131.2 (C-2), 130.6 (C-3), 130.2 × 2 (C-2', 6'), 130.1 (C-1), 128.6 (C-6), 126.8 (C-1'), 115.5 × 2 (C-5, C-9), 111.7 × 2 (C-3', C-5'), 56.0 × 2 (pyrrol-N-CH<sub>2</sub>-CH<sub>2</sub>-CH<sub>2</sub>-CH<sub>2</sub>-N), 47.2 × 2 (piperidone-CH<sub>2</sub>-N-CH<sub>2</sub>), 37.7 (N-CH-Cyclopropyl), 33.7 (C-7), 24.9 × 2 (pyrrol-N-CH<sub>2</sub>-CH<sub>2</sub>-CH<sub>2</sub>-CH<sub>2</sub>-N), 6.4 × 2 (Cyclopropyl(CH<sub>2</sub>-CH<sub>2</sub>)). ESI-MS, *m/z*: 441.4 (M+H)<sup>+</sup>. HRMS (ESI): calcd for C<sub>29</sub>H<sub>32</sub>N<sub>2</sub>O<sub>2</sub> [M+H]<sup>+</sup>: 441.2537, found: 441.2543.

5.1.7.4. (3*E*,5*E*)-3-(3-Allyl-4-hydroxybenzylidene)-1-cyclopropyl-5-[4-(diethylamino) benzylidene]piperidin-4-one (**7d**).

Yellow power. Yield: 25%. m.p.: 175.5–177.3 °C. <sup>1</sup>H NMR (600 MHz, DMSO-*d*<sub>6</sub>) δ (ppm): 9.99 (1H, s, Ar-OH), 7.48 (1H, s, H-β'), 7.47 (1H, s, H-β), 7.34 (2H, d, *J* = 8.4 Hz, H-6', H-2'), 7.20 (1H, d, *J* = 8.4 Hz, H-6), 7.20 (1H, s, H-2), 6.91 (1H, d, *J* = 8.4 Hz, H-5), 6.75 (2H, d, *J* = 8.4 Hz, H-5', H-3'), 6.01–5.95 (1H, m, A-ArCH<sub>2</sub>CH=CH<sub>2</sub>), 5.08–5.04 (2H, m, A-ArCH<sub>2</sub>CH=CH<sub>2</sub>), 3.92 (2H, s, piperidone-CH<sub>2</sub>-N-CH<sub>2</sub>), 3.88 (2H, s, piperidone-CH<sub>2</sub>-N-CH<sub>2</sub>), 3.40 (4H, q, *J* = 7.2 Hz, -N(CH<sub>2</sub>CH<sub>3</sub>)<sub>2</sub>), 3.31 (2H, s, A-ArCH<sub>2</sub>CH=CH<sub>2</sub>), 1.98 (1H, s, -N-CH-Cyclopropyl(CH<sub>2</sub>-CH<sub>2</sub>)), 1.12 (6H, t, *J* = 7.2 Hz, -N(CH<sub>2</sub>CH<sub>3</sub>)<sub>2</sub>), 0.47 (2H, s, -N-CH-Cyclopropyl(CH<sub>2</sub>-CH<sub>2</sub>)), 0.28 (2H, s, -N-CH-Cyclopropyl(CH<sub>2</sub>-CH<sub>2</sub>)). <sup>13</sup>C NMR (150 MHz, DMSO-*d*<sub>6</sub>) δ (ppm): 185.8 (-CO-), 156.3 (C-4), 148.2 (C-4'), 137.4 (C-β), 136.7 (C-β'), 135.7 (C-α), 134.2 (C-α'), 132.9 × 2 (C-2', 6'), 131.1 (C-8), 130.1 (C-2), 129.9 (C-3), 127.7 (C-1), 126.5 (C-6), 126.0 (C-1'), 115.7 (C-5), 115.3 (C-9), 111.2 × 2 (C-3', C-5'), 56.0 × 2 (piperidone-CH<sub>2</sub>-N-CH<sub>2</sub>), 43.7 × 2 (-N(CH<sub>2</sub>CH<sub>3</sub>)<sub>2</sub>), 37.7 (N-CH-Cyclopropyl), 33.5 (C-7), 12.5 × 2 (-N(CH<sub>2</sub>CH<sub>3</sub>)<sub>2</sub>), 6.4 × 2 (Cyclopropyl(CH<sub>2</sub>-CH<sub>2</sub>)). ESI-MS, *m/z*: 443.5 (M+H)<sup>+</sup>. HRMS (ESI): calcd for C<sub>29</sub>H<sub>34</sub>N<sub>2</sub>O<sub>2</sub> [M+H]<sup>+</sup>: 443.2693, found: 443.2719.

5.1.7.5. (3*E*,5*E*)-3-(3-Allyl-4-hydroxybenzylidene)-1-cyclopropyl-5-[4-(dimethyl-amino) benzylidene]piperidin-4-one (**7e**).

Yellow power. Yield: 22%. m.p.: 170.3–172.2 °C. <sup>1</sup>H NMR (600 MHz, DMSO-*d*<sub>6</sub>) δ (ppm): 10.00 (1H, s, Ar-OH), 7.55 (1H, s, H-β'), 7.48 (1H, s, H-β), 7.36 (2H, d, *J* = 8.4 Hz, H-6', H-2'), 7.22 (1H, d, *J* = 7.2 Hz, H-6), 7.21 (1H, s, H-2), 6.91 (1H, d, *J* = 8.4 Hz, H-5), 6.79 (2H, d, *J* = 8.4 Hz, H-5', H-3'), 6.02–5.95 (1H, m, A-ArCH<sub>2</sub>CH=CH<sub>2</sub>), 5.09–5.04 (2H, m, A-ArCH<sub>2</sub>CH=CH<sub>2</sub>), 3.92 (2H, s, piperidone-CH<sub>2</sub>-N-CH<sub>2</sub>), 3.89 (2H, s, piperidone-CH<sub>2</sub>-N-CH<sub>2</sub>), 3.30 (2H, s, A-ArCH<sub>2</sub>CH=CH<sub>2</sub>), 2.99 (6H, s, N-(CH<sub>3</sub>)<sub>2</sub>), 1.98 (1H, s, -N-CH-Cyclopropyl(CH<sub>2</sub>-CH<sub>2</sub>)), 0.47 (2H, s, -N-CH-Cyclopropyl(CH<sub>2</sub>-CH<sub>2</sub>)), 0.27 (2H, s, -N-CH-Cyclopropyl(CH<sub>2</sub>-CH<sub>2</sub>)). <sup>13</sup>C NMR (150 MHz, DMSO-*d*<sub>6</sub>) δ (ppm): 185.81 (-CO-), 156.3 (C-4), 150.7 (C-4'), 136.7 (C-β), 135.5 (C-β'), 134.4 (C-α), 132.8 (C-α'), 132.4 × 2 (C-2', 6'), 131.6 (C-8), 131.034 (C-2), 129.9 (C-3), 128.9 (C-1), 128.7 (C-6), 126.5 (C-1'), 115.7 (C-5), 115.3 (C-9), 111.8 × 2 (C-3', C-5'), 54.9 (piperidone-CH<sub>2</sub>-N-CH<sub>2</sub>), 54.6 (piperidone-CH<sub>2</sub>-N-CH<sub>2</sub>), 48.9 × 2 (N-(CH<sub>3</sub>)<sub>2</sub>), 37.7 (N-CH-Cyclopropyl), 33.5 (C-7), 6.4 × 2 (Cyclopropyl(CH<sub>2</sub>-CH<sub>2</sub>)). ESI-MS, *m/z*: 415.3 (M+H)<sup>+</sup>. HRMS (ESI): calcd for C<sub>27</sub>H<sub>30</sub>N<sub>2</sub>O<sub>2</sub> [M+H]<sup>+</sup>: 415.2380, found: 415.2378.

## 5.2. Animals

The present study was approved by Wenzhou Medical College Animal Policy and Welfare Committee (approval documents: 2013/APWC/0361). Male C57BL/6 mice weighing 18–22 g were obtained from the Animal Center of Wenzhou Medical University (Wenzhou, China). Animals involved in this experiment were treated in accordance with the Guide for Care and Use of Laboratory Animals of National Institutes of Health. The animals were housed in an air-conditioned room and maintained in a 12:12-h light/dark cycle with food and water ad libitum.

## 5.3. Cells and reagents

Lipopolysaccharide (LPS) was obtained from Sigma-Aldrich (St Louis, MO, USA). Saline was prepared as 0.9% NaCl solution. The mouse IL-6 enzyme-linked immunosorbent assay (ELISA) kit and mouse TNF- $\alpha$  ELISA kit were purchased from eBioscience, Inc. (San Diego, CA, USA). Mouse RAW 264.7 macrophages were obtained from the American Type Culture Collection (ATCC, U.S.). RAW 264.7 macrophages were incubated in DMEM medium (Gibco, Eggenstein, Germany) supplemented with 10% FBS (Hyclone, Logan, UT), 100 U/mL penicillin, and 100 mg/mL streptomycin at 37 °C with 5% CO<sub>2</sub>.

## 5.4. Anti-inflammatory evaluation of synthetic MACs

The anti-inflammatory effects of new synthetic allylated MACs were evaluated by inhibition of TNF- $\alpha$  and IL-6 release using in LPS stimulated mouse RAW264.7 macrophages. After treatment of cells with indicated compounds and LPS, the TNF- $\alpha$  and IL-6 levels in medium were determined with an ELISA kit (eBioScience, San Diego, CA) according to the manufacturer's instructions. Briefly, cells were pretreated with 10  $\mu$ M of 8f or prepared symmetric and asymmetric allylated MACs for 30 min, then treated with LPS (0.5  $\mu$ g/mL) for 24 h. After treatment, the culture media and cells were collected separately. The levels of TNF- $\alpha$  and IL-6 in the media were determined by ELISA. The total protein in cultural plates was collected and the concentrations were determined using Bio-Rad protein assay reagents. The total amount of the inflammatory factor in the media was normalized to the total protein amount of the viable cell pellets.

## 5.5. UV-visible absorption spectra of curcumin and its analogs

Absorbance readings were taken from 250 to 600 nm using a spectrum Max M5 (Molecular Devices, USA). A stock solution of 1 mM 8f or allylated MACs was prepared and diluted by phosphate buffer (pH 7.4) to a final concentration of 20 mM. In the experiments where degradation of curcumin was recorded, the absorption spectra were collected for over 25 min at 5 min intervals. The UV-visible absorbance spectrum was measured at 25 °C at varying time interval in a 1 cm path-length quartz cuvette.

## 5.6. Real-time quantitative PCR

Cells were homogenized in TRIZOL kit (Invitrogen, Carlsbad, CA) for extraction of RNA according to each manufacturer's protocol. Both reverse transcription and quantitative PCR were carried out using a two-step M-MLV Platinum SYBR Green qPCR SuperMix-UDG kit (Invitrogen, Carlsbad, CA). Eppendorf Mastercycler ep realplex detection system (Eppendorf, Hamburg, Germany) was used for q-PCR analysis. The primers of genes including TNF- $\alpha$ , IL-6, IL-1 $\beta$ , and VCAM-1 were synthesized by Invitrogen. PCR primers were designed using Primer Premier Version 5.0 software (Premier

Biosoft, Palo Alto, CA, USA) and sequences were as follows (Invitrogen):

TNF- $\alpha$  sense: 5'-TGGAACTGGCAGAAGAGG-3';  
 antisense: 5'-AGACAGAAGAGCGTGGTG-3';  
 IL-6 sense: 5'-GAGGATACCACTCCCAACAGACC-3';  
 antisense: 5'-AAGTGCATCATCGTTGTTCATACA-3';  
 IL-1 $\beta$  sense: 5'-ACTCCTTAGCTCTCGGCCA-3';  
 antisense: 5'-CCATCAGAGGCAAGGAGGAA-3';  
 VCAM-1 sense: 5'-TTTGCAAGAAAAGCCAACATGAAAG-3';  
 VCAM-1 antisense: 5'-TCTCCAACAGTTCAGACGTTAGC-3';  
 $\beta$ -actin sense: 5'-TGGAACTCTGTGGCATCCATGAAAC-3';  
 antisense: 5'-TAAAACGCAGCTCAGTAACAGTCCG-3'.

The amount of each gene was determined and normalized by the amount of  $\beta$ -actin.

## 5.7. Histopathologic examination of lung

Portions of the right lower pulmonary lobe was immersed in 10% neutral-buffered formalin and processed routinely by embedding in paraffin. Sections of tissues were cut at 5  $\mu$ m, mounted on slides, and stained with hematoxylin-eosin before examination under light microscopy (Olympus BH-2; Olympus, Tokyo, Japan). Lung tissues were immersed in 4% paraformaldehyde (PFA), embedded in paraffin, and cut into 5  $\mu$ m thick sections. Tissues were stained with hematoxylin and eosin (H&E) and observed with a Nikon Eclipse E800 microscope (Nikon, Tokyo, Japan). The histologic injury scores were evaluated as Su et al. [24]. Briefly, the severity of microscopic injury was graded according to the following scoring system: 0, normal; 1, minimal (<25%); 2, mild (25%–50%); 3, moderate (50%–75%); and 4, severe (>75%). Tissue sections were examined by an experienced pathologist blinded to treatment.

## 5.8. Wet-to-dry weight ratio

The lung weight-to-dry (W/D) ratio was calculated as a parameter of lung edema. Rats were killed at 6 h after LPS challenge. The upper lobe of right lung was excised, blotted dry, and weighed to obtain the 'wet' weight and then placed in an oven at 65 °C for 48 h to obtain the 'dry' weight. The ratio of the wet lung to the dry lung was calculated to assess the tissue edema.

## 5.9. Protein concentration in bronchoalveolar lavage fluid (BALF)

BALF was obtained at the end of the experimental by irrigating the left lung with saline (3  $\times$  1.5 mL). This fluid was centrifuged at 1000 rpm for 10 min, and the protein concentration in the supernatant was determined using a BCA protein assay (Pierce, Rockford, IL, USA).

## 5.10. Measurement of myeloperoxidase (MPO) activity

The MPO activity was determined by a commercially available assay kit (Jiancheng Bioengineering Institute, Nanjing, China) following the manufacturer's instruction. In brief, the right posterior lobe lungs were removed from rats of all groups and MPO activity was measured. One hundred milligrams of lung tissue was homogenized and fluidized in extraction buffer to obtain 5% of the homogenate. The sample including 0.9 mL homogenate and 0.1 mL of reaction buffer was heated to 37 °C in a water bath for 15 min, and then the enzymatic activity was determined by measuring the changes in absorbance at 460 nm using a 96-well plate reader. One unit of MPO was defined as that giving an increase in absorbance of

0.001 per min and specific activity was given as units/mg protein.

### 5.11. Experimental logP evaluation

Octanol (300 mL) and water (1200 mL) was saturated with each other on Thermostat Shaker (28 °C) for 3 days in 180 r/min. After 3 days, the two layer was extracted and put into different bottles, respectively. Compounds (1.0 mg/mL, dissolved in extractive octanol) were diluted into six different concentrations, including 30 µg/mL, 25 µg/mL, 20 µg/mL, 15 µg/mL, 10 µg/mL and 5 µg/mL. The different solutions were mixed with methanol (v/v, 1:4), respectively, and then, the standard curve of Absorbance-Concentration was determined by microplate reader of compounds ( $\lambda_{\max} = 405 \text{ nm}$ ,  $R^2 \geq 0.99$ ). Compounds (10 µg/mL) were mixed with water (v/v, 1:10) in 15 mL-centrifuge tube (repeat for 3 times), then these three tubes were shook in Thermostat Shaker (28 °C) for 2 h in 180 r/min. The OD value in octanol layer was detected by microplate reader of compounds, and the concentration in octanol ( $C_{(\text{octanol})}$ ) of different tubes were calculated by the standard curve of Absorbance-Concentration, so the final LogP value could be calculated by a LogP calculation formula ( $\text{LogP} = \text{Log}(C_{(\text{octanol})} \times V_{(\text{water})}) / (C_0 \times V_0 - C_{(\text{octanol})} \times V_{(\text{octanol})})$ ),  $C_0$  means the original concentration in octanol of compounds,  $V_0$  means the original volume in octanol of compounds), the evaluation of LogP in three tubes should be closely.

### 5.12. Cytokine assays

The concentrations of cytokine IL-6 and TNF- $\alpha$  in the supernatants of the BALF were measured by enzyme-linked immunosorbent assay (ELISA) using commercially available reagents according to the manufacturer's instructions (eBioscience, San Diego, CA, USA).

### 5.13. Statistical analysis

Results are expressed as the mean  $\pm$  standard error of the mean (SEM). Student's t-test was employed to analyze the differences between sets of data. Statistics were performed using GraphPad Pro (GraphPad, San Diego, CA). P values less than 0.05 ( $p < 0.05$ ) were considered indicative of significance. All experiments were repeated at least three times.

### Acknowledgement

Financial support was provided by the National Natural Science Funding of China (21472142, 21572167), Zhejiang Natural Science Funding (LQ15B020005), Scientific Research Foundation of Wenzhou Medical University (QTJ13003), Public Welfare Science and Technology Project of Wenzhou (Y20140736), and the Project-sponsored by SRF for ROCS, SEM.

### Appendix A. Supplementary data

Supplementary data related to this article can be found at <http://dx.doi.org/10.1016/j.ejmech.2016.05.041>.

### References

[1] H. Lakshminarayana Pradeep, M. Kahn Jeremy, First do no harm: surrogate

- endpoints and the lesson of  $\beta$ -agonists in acute lung injury, *Crit. Care* 16 (2012) 314.
- [2] S. Zhang, S.D. Danchuk, R.W. Bonvillian, B. Xu, B.A. Scruggs, A.L. Strong, J.A. Semon, J.M. Gimble, A.M. Betancourt, D.E. Sullivan, B.A. Bunnell, Interleukin 6 mediates the therapeutic effects of adipose-derived stromal/stem cells in lipopolysaccharide-induced acute lung injury, *Stem. Cells* 32 (2014) 1616–1628.
- [3] A. Dushianthan, M.P. Grocott, A.D. Postle, R. Cusack, Acute respiratory distress syndrome and acute lung injury, *Postgrad. Med. J.* 87 (2011) 612–622.
- [4] H.C. Do-Umehara, C. Chen, D. Ulrich, L. Zhou, J. Qiu, S. Jang, A. Zander, M.A. Baker, M. Eilers, P.H. Sporn, K.M. Ridge, J.L. Sznajder, G.R. Budinger, G.M. Mutlu, A. Lin, J. Liu, Suppression of inflammation and acute lung injury by Miz1 via repression of C/EBP- $\delta$ , *Nat. Immunol.* 14 (2013) 461–469.
- [5] T.H. Cao, S.G. Jin, D.S. Fei, K. Kang, L. Jiang, Z.Y. Lian, S.H. Pan, M.R. Zhao, M.Y. Zhao, Artesunate protects against sepsis-induced lung injury via heme oxygenase-1 modulation, *Inflammation* 39 (2016) 651–662.
- [6] J.W. Lee, X. Fang, A. Krasnodemska, J.P. Howard, M.A. Matthay, Concise review: mesenchymal stem cells for acute lung injury: role of paracrine soluble factors, *Stem. Cells* 29 (2011) 913–919.
- [7] B.B. Aggarwal, B. Sung, Pharmacological basis for the role of curcumin in chronic diseases: an age-old spice with modern targets, *Trends Pharmacol. Sci.* 30 (2009) 85–94.
- [8] K. Suda, M. Tsuruta, J. Eom, C. Or, T. Mui, J.E. Jaw, Y. Li, N. Bai, J. Kim, J. Man, D. Ngan, J. Lee, S. Hansen, S.W. Lee, S. Tam, S.P. Man, S. Van Eeden, D.D. Sin, Acute lung injury induces cardiovascular dysfunction: effects of IL-6 and budesonide/formoterol, *Am. J. Respir. Cell Mol. Biol.* 45 (2011) 510–516.
- [9] E.R. Johnson, M.A. Matthay, Acute lung injury: epidemiology, pathogenesis, and treatment, *J. Aerosol. Med. Pulm. Drug Deliv.* 23 (2010) 243–252.
- [10] Koh Younsuck, Update in acute respiratory distress syndrome, *J. Intensive Care* 2 (2014) 2–6.
- [11] R.C. Srimal, B.N. Dhawan, Pharmacology of diferuloyl methane (curcumin), a non-steroidal anti-inflammatory agent, *J. Pharm. Pharmacol.* 25 (1973) 447–452.
- [12] D. Sun, X. Zhuang, X. Xiang, Y. Liu, S. Zhang, C. Liu, S. Barnes, W. Grizzle, D. Miller, H.G. Zhang, A novel nanoparticle drug delivery system: the anti-inflammatory activity of curcumin is enhanced when encapsulated in exosomes, *Mol. Ther.* 18 (2010) 1606–1614.
- [13] B.B. Aggarwal, K.B. Harikumar, Potential therapeutic effects of curcumin, the anti-inflammatory agent, against neurodegenerative, cardiovascular, pulmonary, metabolic, autoimmune and neoplastic diseases, *Int. J. Biochem. Cell Biol.* 41 (2009) 40–59.
- [14] R. Wilken, M.S. Veena, M.B. Wang, E.S. Srivatsan, Curcumin: a review of anticancer properties and therapeutic activity in head and neck squamous cell carcinoma, *Mol. Cancer* 10 (2011) 1–19.
- [15] M.M. Yallapu, S. Khan, D.M. Maher, M.C. Ebeling, V. Sundram, N. Chauhan, A. Ganju, S. Balakrishna, B.K. Gupta, Na Zafar, M. Jaggi, S.C. Chauhan, Anticancer activity of curcumin loaded nanoparticles in prostate cancer, *Bio-materials* 35 (2014) 8635–8648.
- [16] J. Yan, Y. Wang, X. Zhang, S. Liu, C. Tian, H. Wang, Targeted nanomedicine for prostate cancer therapy: docetaxel and curcumin co-encapsulated lipid-polymer hybrid nanoparticles for the enhanced anti-tumor activity in vitro and in vivo, *Drug Deliv.* 27 (2015) 1–6.
- [17] E. Burgos-Moron, J.M. Calderon-Montano, J. Salvador, A. Robles, M. Lopez-Lazaro, The dark side of curcumin, *Int. J. Cancer* 126 (2010) 1771–1775.
- [18] P. Anand, A.B. Kunnumakkara, R.A. Newman, B.B. Aggarwal, Bioavailability of curcumin: problems and promises, *Mol. Pharm.* 4 (2007) 807–818.
- [19] Z. Liu, L. Tang, P. Zou, Y. Zhang, Z. Wang, Q. Fang, L. Jiang, G. Chen, Z. Xu, H. Zhang, G. Liang, Synthesis and biological evaluation of allylated and prenylated mono-carbonyl analogs of curcumin as anti-inflammatory agents, *Eur. J. Med. Chem.* 74 (2014) 671–682.
- [20] Z. Liao, J. Dong, W. Wu, T. Yang, T. Wang, L. Guo, L. Chen, D. Xu, F. Wen, Resolvin D1 attenuates inflammation in lipopolysaccharide-induced acute lung injury through a process involving the PPAR $\gamma$ /NF- $\kappa$ B pathway, *Respir. Res.* 13 (2012) 110.
- [21] J.L. Goldman, S. Sammani, C. Kempf, L. Saadat, E. Letsiou, T. Wang, L. Moreno-Vinasco, A.N. Rizzo, J.D. Fortman, J.G. Garcia, Pleiotropic effects of interleukin-6 in a “two-hit” murine model of acute respiratory distress syndrome, *Pulm. Circ.* 4 (2014) 280–288.
- [22] E. Dreassi, A.T. Zizzari, F. Falchi, S. Schenone, A. Santucci, G. Maga, M. Botta, Determination of permeability and lipophilicity of pyrazolo-pyrimidine tyrosine kinase inhibitors and correlation with biological data, *Eur. J. Med. Chem.* 44 (2009) 3712–3717.
- [23] J. Bones, K.V. Thomas, B. Paull, Using environmental analytical data to estimate levels of community consumption of illicit drugs and abused pharmaceuticals, *J. Environ.* 9 (2007) 701–707.
- [24] X. Su, L. Wang, Y. Song, C. Bai, Inhibition of inflammatory responses by ambroxol, a mucolytic agent, in a murine model of acute lung injury induced by lipopolysaccharide, *Intensive. Care. Med.* 30 (2004) 133–140.